

# **Learning The-Self: Leveraging Proprioception to Guide the Autonomous Discovery of the Robotic Body Schema**

Fernando Díaz Ledezma, M.Sc.

**Ph.D. Thesis**



**TECHNISCHE UNIVERSITÄT MÜNCHEN**  
**Munich Institute of Robotics and Machine Intelligence**

**Learning The-Self: Leveraging Proprioception to  
Guide the Autonomous Discovery of the Robotic  
Body Schema**

Fernando Díaz Ledezma, M.Sc.

Vollständiger Abdruck der von der TUM School of Computation, Information and Technology der Technischen Universität München zur Erlangung des akademischen

Grades eines

Doktor-Ingenieurs (Dr.-Ing.)

genehmigten Dissertation.

Vorsitzender: Prof. Dr. XXX

Prüfer der Dissertation: 1. Prof. Dr.-Ing. Sami Haddadin

2. Prof. XXX

3. Prof. XXX

Die Dissertation wurde am **XX.XX.2024** bei der Technischen Universität München eingereicht und durch die TUM School of Computation, Information and Technology am **XX.XX.2024** angenommen.

I am not Ultron, I am not Jarvis, I  
am... I am.

---

*Vision, Avengers: Age of Ultron*



# Abstract

As robots become increasingly integral to human life, the imperative emerges for them to autonomously explore and construct models of their bodies. Robots should take cues from human capabilities, aspiring to build and utilize their body schema for advanced locomotion, finer manipulation, and adaptive interactions. Thus, a crucial foundation lies in seamlessly integrating the body schema to elevate learning, motor control, coordination, and spatial awareness. Furthermore, future robots should become self-sufficient entities that conduct monitoring, calibration, and adaptation exclusively through onboard sensing modalities. Standardizing constant self-monitoring nurtures spatial awareness and facilitates rapid error detection and correction. A profound understanding of their body structure will undoubtedly lead to enhanced, safe, and energy-aware interactions. However, current robot learning approaches encounter limitations, such as suboptimal generalization and sample efficiency, exhibiting a need for more structural knowledge. Versatile methods, like neural networks, confront challenges related to data and topology, confining learning to specific regions. On the other hand, learning robot physical attributes still rely on a presumed knowledge of the mechanical topology, often involving calibration and offline identification in controlled environments with a persistent reliance on external measurements, such as vision and motion-capturing systems. The research landscape generally reveals the lack of a unified framework that enables robots to build representations of their body schema to achieve improved body awareness and interaction capabilities. This study addresses these challenges by consolidating necessary and sufficient proprioceptive signal quantities, enabling robots to autonomously acquire knowledge about their body structure without relying on exteroceptive off-body sensors. It introduces an approach that reformulates robot kinematic calibration and system identification as a modular computational graph amenable to machine learning. This abstracted architecture, applied in online learning phases, seamlessly merges proprioceptive signals with first-order principles, extracting fundamental features of the robot body schema. Characterizing morphological properties of tree-like structures, the study infers mechanical topology through information-theoretic measures, validating and applying it independently of off-robot calibration. The research extends its scope by complementing the robot body schema by instantiating inertial properties, ensuring on-

line learning and physical feasibility. Ultimately, this work challenges the uncritical application of end-to-end learning in physical systems, urging a reevaluation of its limitations when excluding principled knowledge. It underscores opportunities for machine learning frameworks in embodied systems, emphasizing the untapped potential of synergizing structural knowledge with data-driven methods. This study catalyzes future research in an incipient field that underscores building and maintaining a body schema by demonstrating that fundamental properties of a robot's morphology can be deduced from proprioceptive signals. Its implications are far-reaching, addressing the needs of conventional and dynamic robotic structures with diverse sensory modalities that require a more profound sense of self.

# Contents

<b>1</b>	<b>Introduction</b>	<b>1</b>
1.1	Motivation and vision . . . . .	3
1.2	Problem Statement . . . . .	6
1.3	Research Questions and Contribution . . . . .	7
1.4	State of the Art . . . . .	7
1.5	Thesis Structure . . . . .	7
1.6	Curriculum Vitae . . . . .	7
<b>2</b>	<b>Related Work</b>	<b>9</b>
2.1	Model learning in robotics . . . . .	10
2.1.1	End-to-end learning . . . . .	10
2.2	Data-driven learning with structure information . . . . .	11
2.3	Model learning and the body schema . . . . .	12
2.4	Model learning in robotics . . . . .	13
2.4.1	Classical and recent works in system identification . . . . .	13
2.4.2	Local and global models linear models . . . . .	13
2.4.3	End-to-end learning (black box models) . . . . .	13
2.5	Data-driven learning with structure information . . . . .	13
2.6	Model learning and the body schema . . . . .	13
2.6.1	Internal representations . . . . .	13
2.6.2	Sensorimotor maps . . . . .	13
<b>3</b>	<b>Theoretical Foundations</b>	<b>15</b>
3.1	Introduction . . . . .	15
3.2	Different views on the body and its features . . . . .	16
3.2.1	The physical self . . . . .	16
3.2.2	Summary of the body concepts . . . . .	18
3.3	The robot body schema . . . . .	19
3.3.1	Properties of the body schema . . . . .	19

3.4	Robotics and the properties of the body schema . . . . .	21
3.4.1	Perceiving the body: Robot proprioception . . . . .	21
3.4.2	Modeling body size, position, and posture: Robot kinematics . . . . .	22
3.4.3	The inertial properties of the body schema . . . . .	28
3.4.4	Describing body shape: Robot mechanical topology . . . . .	33
3.4.5	Learning and adaption of the body properties . . . . .	44
3.5	Chapter summary . . . . .	50
<b>4</b>	<b>Methods: How to learn the robotic body schema</b>	<b>51</b>
<b>5</b>	<b>Results</b>	<b>53</b>
<b>6</b>	<b>Discussion</b>	<b>55</b>
	<b>Bibliography</b>	<b>55</b>

# Abbreviations and Symbols

In this thesis, scalar quantities are written as plain letters, e.g.,  $\lambda$ ,  $c$ ,  $K$ . Vectors and matrices are represented by bold letters, whereas vectors have small letters, e.g.,  $q$ ,  $\theta$  and matrices capital letters  $K$ ,  $M$ . The total derivative w.r.t. time is indicated by a dot above the symbol, i.e.,  $\dot{x} = \frac{d}{dt}x$ ,  $\ddot{x} = \frac{d^2}{dt^2}x$ . The Euclidian norm of a vector  $q$  is denoted by  $|q|$ , the dot product of two vectors  $a$  and  $b$  by  $(a, b)$  and their cross product by  $a \times b$ .

All symbols are introduced in the text before they are used. In some sections, the argument is omitted for brevity. Several variables appear with different subscripts, superscripts, additional symbols and dimensions. In the following list, the quantities are generally described without being further specified. The specific meaning becomes apparent when the respective variable is introduced in the text. Please note that the list of symbols is not complete, but it contains symbols that appear frequently or are of major importance in this thesis.

## List of Symbols

### General Symbols

$q$	Joint positions
$\dot{q}$	Joint velocities
$\ddot{q}$	Joint acceleration
$T$	Pose in matrix form
$T_d$	Desired pose in matrix form
$x$	Pose in vector form
$x_d$	Desired pose in vector form
$\dot{x}$	Twist
$\dot{x}_d$	Desired twist

$\ddot{x}$	Cartesian acceleration
$\ddot{x}_d$	Desired Cartesian acceleration
$f$	Wrench
$f_d$	Desired wrench
$f_{ff}$	Feed-forward wrench
$f_{\text{ext}}$	External wrench
$\tau$	Joint motor torques
$\tau_d$	Desired joint motor torques
$\tau_{\text{ext}}$	External joint torque
$K_x$	Cartesian stiffness
$K$	Joint stiffness
$D_x$	Cartesian damping
$D$	Joint damping
$J_x$	Jacobian
$M$	Mass matrix
$C$	Coriolis vector
$g$	Gravity vector
$t$	Time
$\mathcal{U}(\cdot)$	Environment around a pose

## Process, Tactile Skill, and Taxonomy

$\varsigma$	Skill
$\iota$	Task
$\pi_d$	Tactile policy
$\Pi$	Set of tactile policies
$p$	Process
$\mathcal{P}$	Set of processes
$\mathcal{T}$	Taxonomic synthesis algorithm

$o$	Object
$\mathcal{O}$	Set of objects
$s$	Process state
$s_0$	Initial process state
$s_1$	Final process state
$s_e$	Error process state
$s_\pi$	Policy process state
$\mathcal{C}_{\text{pre}}$	Process pre condition
$\mathcal{C}_{\text{err}}$	Process error condition
$\mathcal{C}_{\text{suc}}$	Process success condition
$\delta$	Process step transition
$\Delta$	Set of process step transition
$\theta$	Parameters
$\theta_\pi$	Skill parameters
$\theta_c$	Controller parameters

## GGTWreP framework

$w$	World state
$\mathcal{W}$	World state space
$E$	Effects of skill execution on environment
$\mathcal{R}$	Requirements for skill execution
$\mathbb{D}$	Parameter domain
$\mathbb{C}$	Skill constraints
$\mathfrak{D}$	Dataset from a learning experiment
$\mathcal{Q}$	Quality metric
$\mathcal{C}$	Tactile policy commands

## Planning

$\mathcal{A}$	Assembly
$\rho$	Assembly part
$\Gamma$	Set of assembly parts
$a$	Assembly action
$\alpha$	Sequence of assembly actions
$w$	Agent
$W$	Set of agents
$\zeta$	Assembly state
$\mathcal{Z}$	Set of assembly states

## Abbreviations

ADAM	Adaptive Momentum
AI	Artificial intelligence
CGL	Combinatorial graph Laplacian
DL	Deep learning
DOF	Degrees of freedom
EE	End effector
e.g.	<i>Exemplis grata</i> (for example)
ESN	Echo state network
etc.	<i>Et cetera</i> (and so forth)
F/T sensor	Force/torque sensor
GD	Gradient descent
GP	Gaussian process
ICRA	International Conference on Robotics and Automation
i.e.	<i>Id est</i> (that is)
IEEE	Institute of Electrical and Electronics Engineers

LbD	Learning by demonstration
LWR	Lightweight Robot
MI	Mutual information
MIRMI	Munich Institute of Robotics and Machine Intelligence
ML	Machine learning
MST	Maximum spanning tree
NTI	Network topology inference
ODE	Ordinary differential equation
PC	Personal Computer
RL	Reinforcement Learning
ROI	Region of interest
ROS	Robot Operating System
SPD	Symmetric Positive Definite
SVM	Support vector machine
TMI	Total mutual information
TUM	Technical University Munich
UAV	Unmanned aerial vehicle
w.r.t.	With respect to



# 1

## Introduction

Imagine your body; do not look at it. Close your eyes and tell me what you see. What is the pose of your body right now? Are you standing, seated, lying? Where are your arms and hands? Do not open your eyes just yet. Now, touch your left knee with your right hand. Did you struggle to find your knee? Chances are you did not. How can we manage to know where our body parts are in space at all times without even looking at them? It is safe to assume that we humans have what is called an internal model of our physical self. That is, we have a representation of our body. Such a representation allows us to accomplish remarkable feats. Have you ever caught an object in mid-air? Certainly, succeeding in that involved not only estimating the trajectory of the object but also the motion that your arm and hand needed to accomplish to reach the catching point. Had your arm dimensions been different from the ones you *have in mind*, or had the accuracy of your knowledge about your arm's pose been insufficient, you would not have caught the object. This internal model of yourself is called the body schema in psychology and neuroscience. It plays a definite role in knowing about the state of our body in space and also in calculating how we move. Consider a different scenario. You are in a pool and have been floating around for quite some time now. By the time you leave the pool, you feel heavier, like you need to put more effort into moving your body. A similar example happens during a workout at the gym. You lift a heavy dumbbell for a number of repetitions, and then, when you are done, it feels like bending your arm takes no effort at all. Your body schema adapted its representation to the situation. The accuracy of this internal model and, certainly, its plasticity play an important role in the kinematic and

dynamic control of our bodies. Not only that, but the schema is very much related to our ability to use tools, say a pencil, a hammer, or a golf club. Our body schema is plastic and can temporarily integrate external objects, giving us the capability to manipulate those tools with such dexterity as if they were parts of our own bodies.

Robots have been driving mass production in industries for a good number of decades. They are an essential part of assembly lines in factories. Teams of them take care of tasks demanding high precision. Yet, even as they have been undoubtedly the workforce of automation, they are not as autonomous as we would like them to be. They are designed, constructed, and programmed to be accurate. To really ensure accuracy in their tasks, it is not only the robots that need to move with high precision, but also their environments need to be controlled. Every possibility of interaction needs to be predefined, and disturbances are to be minimized if not completely eliminated. This is precisely the reason why robots in industries normally execute their tasks in confined spaces, having little or no interaction at all with the external environments, let alone with humans. However, in recent decades, there has been a shift. Technology has evolved enough so that robots are now leaving these enclosed and protected environments and are aiming at increased interaction with their surroundings, other robots, and people. This advanced interaction comes at a price: uncertainty. The world cannot be modeled; every single potential interaction scenario cannot be anticipated and controlled. Robots, if they are to succeed in the human world, need to improvise strategies, adapt to the situation, and overcome constant, ever-changing challenges. But robots are not (at least until now) adaptable; the ways in which they are modeled are fixed and rarely subject to change. Their control paradigms also do not account for changes. Naturally, their very own bodies are not supposed to change. But change is there, a constant factor. Wear and tear is a typical phenomenon. A localized malfunction is an event that, although undesired, could occur, and a robot should be able to handle it. Perhaps the task that it needs to execute has parameters slightly different from what was anticipated; tools could be different, and the environment could be different. To put it bluntly, modern robots need to have plasticity in their models, just as humans do.

Let us go back to our imagination. Say you are left-handed. Unfortunately, you had a light accident and broke your left arm. Nothing serious, but you will not be using that arm for a couple of weeks. You can adapt your internal model to account for this situation and will probably become dexterous with that good right arm. If a humanoid robot is programmed to accomplish tasks with both arms and one ceases to operate for some reason, it is unlikely that it will carry on with the task. At this point, the engineers responsible for this robot may determine that the robot can be repurposed while the arm is repaired. They adapt the model of the robot, tune some parameters, and off the robot goes to work on its new tasks. But this is not the level of autonomy we imagine when we see a future in which robots coexist with us and assist us in a myriad of things. Once again, robots need to adapt. And the very first

aspect that needs to be adapted is their own body. For that, robots need to have the capability to understand and construct a model of their bodies. This brings back the discussion to the idea that a robot can certainly benefit from the understanding of its physical self, and for that, it would need to leverage information coming from its on-board sensors and fuse them with ground truths to make sense of its body and the world around it. But how?

## 1.1 Motivation and vision

**Empowering Robots to Learn and Control their Bodies** As the integration of robots into various facets of human life becomes more pronounced, there arises a crucial imperative for these machines to proactively participate in the exploration and development of models for their own bodies. At the core of this autonomous self-discovery is the development of an awareness of the physical self by developing and maintaining a body schema. This self-awareness represents a pivotal step towards endowing robots with a profound understanding of their own embodiment and becomes the foundation for the integration of sensory information and motor control. The robot body schema, akin to the internal representation of the human body in the brain, becomes a dynamic and evolving map that serves as a reference point for the robot's interactions with its surroundings. The establishment of a body schema contributes significantly to the enhancement of robot motor control. Robots, equipped with a coherent internal model of their bodies, can execute movements with a heightened level of precision and coordination. The fusion of sensory information and motor control within the body schema lays the scaffolding for efficient learning. Additionally, autonomous self-discovery is not a static process. It involves ongoing refinement and adaptation. As robots encounter diverse environments and engage in various tasks, their body schema adapts and expands, allowing for an extended understanding of their physical capabilities. This adaptability is crucial for robots to navigate the intricacies of real-world scenarios, adjusting their responses based on the context in which they operate. The significance of this autonomous self-discovery transcends the technical aspects of robotics; it resonates with the broader narrative of robots becoming integrated and adaptive participants in human-centric environments. By actively engaging in the exploration of their own bodies, robots pave the way for a future where they seamlessly navigate, interact, and adapt in tandem with human activities. This not only enhances their functional capabilities but also fosters a harmonious integration of robots into diverse and dynamic human-centric spaces.

**Learning and the body schema** The seamless integration of the body schema is indispensable for the evolution of robots, forming the foundational underpinning upon which multifaceted capabilities are constructed. This integration spans across various domains, encompassing learning for physical awareness, motor control, coordination, and interaction.

Learning, a hallmark of intelligent systems, coexists in a dual relationship with the body schema: learning not only contributes to the development of the body schema but, reciprocally, the body schema enhances learning. Primarily, it plays a pivotal role in detecting the structure within the myriad afferent and efferent signals of the robot's sensorimotor system, facilitating the construction of the body schema. Simultaneously, the incorporation of the body schema into learning frameworks allows robots to explore their sensorimotor maps and develop models of their morphology. This understanding becomes a scaffold for acquiring new skills, refining existing ones, and assimilating knowledge gained from interactions with the environment. The integration of the body schema thus catalyzes a learning process that is not only adaptive but also inherently tied to the robot's physical embodiment. Moving to motor control, another pivotal aspect of intelligent systems, there exists an intricate link to learning the body schema. Internal body representations that can adapt through learning mechanisms contribute to the development of superior forward and inverse models, ultimately refining control precision. Lastly, a seamlessly integrated body schema empowers robots to learn diverse tasks, surpassing the limitations of rigid, pre-programmed functionalities. Ultimately, a plastic body representation provides versatility crucial in dynamic and unpredictable settings, where the cohesive ability to learn, control movements, coordinate actions, and perceive space allows robots to thrive in a myriad of scenarios.

**Enhancing locomotion, manipulation, and adaptability.** Taking inspiration from the nuanced abilities of humans, the vision for future robots is set to take advantage of the enhanced bodily awareness that the integration of a body schema will bring about, thereby improving adaptability and interaction in diverse situations. The development and maintenance of the robot body schema will unlock a spectrum of capabilities that enables precise and coordinated movements, fostering in particular advanced locomotion, motion planning, and intricate manipulation. Bodily awareness is expected to revolutionize the locomotive prowess of robots. Future machines, informed by this internal map of their physical structure, will navigate environments with an unprecedented level of sophistication. This extends beyond basic movement, enabling robots to traverse complex terrains, negotiate obstacles, and adapt seamlessly to changes in their surroundings. Motion planning, a core element of robotics, will harness the robot body schema as a dynamic blueprint, supporting not only precise and efficient movements but also the ability to determine near-optimal trajectories in real-time. The result is a more adaptive and resourceful approach to navigating intricate spaces and executing tasks with heightened precision. The mastery of a body schema extends to manipulation with profound implications. Future robots, leveraging this internal map, will exhibit a level of dexterity and precision in manipulating objects that mirrors the intricacies of human hand-eye coordination. This enhanced capability will represent a breakthrough in applications requiring delicate and precise interactions, from han-

dling diverse items to executing complex manufacturing tasks. Moreover, coordination and collaboration with other robots or humans becomes more refined through a well-integrated body schema, as it allows robots to anticipate and adapt their interactions with other agents. This anticipatory and adaptive capability is fundamental for fostering safe, effective, and harmonious interactions.

**Constant self-monitoring for autonomy** Continuous self-monitoring signifies a fundamental imperative for future robotic systems. It is achieved through the amalgamation of internal models and the uninterrupted stream of sensorimotor signals. This seamless fusion enables a dynamic and real-time understanding of the robot's own state, creating a powerful feedback loop that is integral to the system's autonomy. Perpetual monitoring sets in motion successive phases of error detection and correction. This iterative process ensures that the robot is not only aware of its physical state but also capable of recognizing and rectifying discrepancies between intended actions and actual outcomes. The ability to identify errors in real-time positions future robots on a trajectory towards enhanced reliability and precision in its interactions. The profound impact of this ongoing adaptation is most evident in the rapid formulation and execution of contingency motion strategies. Armed with an enriched spatial awareness and a continuously evolving set of internal models, the robot becomes adept at anticipating and responding to unforeseen challenges. In dynamic and unpredictable environments, the ability to swiftly devise and implement contingency plans allows the robot to navigate complex scenarios with agility and efficiency. This advanced interaction capability with the environment is a hallmark of the paradigm of continuous self-monitoring. The robot not only perceives its surroundings in real-time but also possesses the foresight to proactively engage with its environment. This goes beyond mere reactionary responses; it encapsulates a proactive and intelligent engagement that significantly elevates the robot's efficacy in accomplishing tasks and navigating diverse scenarios.

**Onboard sensing for self-sufficiency** Achieving true autonomy requires robots to evolve into self-sufficient entities capable of independent learning, calibration, monitoring, and adaptation of their body representation. This transformation is predicated on the exclusive reliance on onboard sensing modalities, a fundamental transition that empowers robots with heightened versatility and adaptability. At the core of this self-sufficiency lie two fundamental sensory modalities: somatosensation, encompassing proprioception and touch, and vision. These modalities collectively provide the robot understanding of its own body and the surrounding environment. Proprioception provides the robot awareness of its own body in space. The sense of touch complements the understanding of the body and allows the robot to distinguish itself from its immediate environment. Vision, another cornerstone modality, extends the robot's perception beyond immediate physical contact. By abstaining

from off-board sensing devices, robots liberate themselves from external dependencies and enhance their self-sufficiency. Leveraging onboard sensing modalities empowers robots to dynamically respond to changes in their surroundings in real-time. Whether it's navigating through a cluttered environment, adjusting movements for safety, or adapting to unforeseen obstacles, the reliance on somatosensation and vision will enable future robot to operate with a level of autonomy and adaptability previously unseen.

**Safety- and energy-awareness** Comprehending their own body structure empowers robots to engage in more effective and nuanced interactions with both their robotic and human counterparts. The body schema serves as a predictive tool, endowing robots with the foresight to anticipate potential challenges. This heightened understanding facilitates dynamic adjustments in their movements, prioritizing safety and fostering efficiency in diverse collaborative scenarios. When interacting with other robots, this capability enables seamless coordination, averting collisions or disruptions during joint tasks. Likewise, in human-robot interactions, the ability to adapt movements ensures a safer environment, mitigating the risk of accidental impacts or collisions. Moreover, the comprehension of their own body structure provides robots with a unique advantage in optimizing energy consumption. By adapting their motions based on the inherent physical properties of their structures, robots can execute tasks with greater efficiency. This optimization is particularly crucial in mobile robotics, where energy conservation is paramount given the limited resources. The dual capability of enhancing safety in interactions and contributing to energy-aware robotics underscores the significance of robots understanding their own body structure in fostering a more efficient, collaborative, and environmentally conscious robotic landscape.

## 1.2 Problem Statement

Navigating the complexities of learning a robot's physical attributes in the field of robotics reveals intricate challenges that demand a closer look. Traditional calibration routines, tailored for known kinematic structures and offline system identification methods, face limitations concerning generalization capabilities, sample efficiency, and the reliance on a pre-determined mechanical topology. This is particularly evident in the context of global and local machine learning frameworks for physical systems, where the exclusion of structural knowledge often results in operational inefficiencies.

Compounding these challenges is the substantial reliance on off-robot measurement devices, such as vision and motion-capturing systems, during calibration and identification processes. Despite the wealth of sensor signals from modern robots, determining the minimum set required for constructing a body model based solely on robot sensing remains a persistent and unresolved challenge. This dependence on external measurements not only

introduces limitations but also raises questions about the practicality and applicability of learned models in real-world scenarios.

Venturing into alternative learning methods, such as neural networks, introduces a unique set of challenges. These approaches frequently lack crucial information about the robot's body structure, necessitating vast amounts of data for effective learning. The design of neural networks further compounds the issue, as it becomes an expert-driven task requiring meticulous determination of topology. Often, these approaches suffer from generalization limitations, confining their learning capabilities to specific input-output regions.

Examining the research landscape reveals substantial gaps, including an unclear understanding of how object handling extends the robotic body schema. Furthermore, limited exploration into the mechanical arrangement of joints and links, known as the mechanical topology, underscores untapped potential in understanding the intricate details of robotic physical structure. These research gaps collectively contribute to the overarching challenge of lacking a unifying scheme that seamlessly integrates all learning stages, hindering the development of a fully characterized robotic body schema based solely on knowledge about sensorimotor signals.

To address these multifaceted challenges effectively, there is a compelling need to bridge the existing gaps and explore innovative learning approaches. This includes the development of methods capable of incorporating structural knowledge, reducing reliance on external measurements, and enhancing the generalization capabilities of machine learning frameworks in the realm of robotics. Moreover, the establishment of a comprehensive unifying scheme stands as a pivotal step toward advancing the field and achieving a fully characterized robotic body schema.

### **1.3 Research Questions and Contribution**

### **1.4 State of the Art**

### **1.5 Thesis Structure**

### **1.6 Curriculum Vitae**



# 2

## Related Work

One fundamental characteristic of humans is the awareness of the body, which allows its control with dexterity and plasticity. We know where our body is in space, we know much of that space our body takes, and we know how to take it from its present situation at time  $t$ , its current *state*  $s_t$ , to a predicted or expected future state  $s_{t+1}$  at time  $t + 1$  given a carefully chosen *action*  $a_t$ . The ability to anticipate the future and to determine the actions that can take us there is connected to the notions of forward and inverse models in cognitive science and robotics [1–3]. An alternative and complementary interpretation is that of sensorimotor contingencies [4–6], which denote the structured relations between the actions of an agent and the ensuing sensory inputs resulting from interaction. The potential sensorimotor interactions are connected to the concept of *embodiment*, which, as expressed by Pfeifer et al. [7], deals with “how the body shapes the way we think,” putting a premium on the morphology and capacities of an agent. Last, a few strongly related concepts are pertinent to the discussion: the *ecological self* [REFERENCE](#), the *physical self* [REFERENCE](#), and the *body schema* [REFERENCE](#). They are different interpretations of *body models* that describe its physical structure and capabilities, and integrate sensory information for prediction and action. Research in cognitive science tells us that we construct and maintain representations involving the previous concepts from the moment that we are in womb and during all our conscious existence. Maintaining those models is not only a matter of refining and tuning them but also may involve adapting them to accommodate unexpected drastic changes. The level of bodily awareness encoded in those representations allows to achieve remarkable

feats, like reach for things without even looking, catching an object in midair, or contorting our bodies to maneuver in tight spaces or negotiate obstacles.

As discussed in the Introduction the vision for future robots involves giving them bodily awareness capabilities inspired in humans. To contextualize what is the state of the art towards realizing that vision, this chapter provides a review and discussion of relevant works that address the field of modeling in robotics; in particular, model learning. The discussion will include a brief review of the fundamental methods to model robots and will gradually move to the paradigm of learning local and global models with and without prior knowledge. The discussion will connect with the above mentioned concepts pertaining body models and present pertinent works that have presented methods to learn the body schema and sensorimotor representations in robotics

**It is also important to emphasize internal models for awareness [8]**

## 2.1 Model learning in robotics

Existing learning frameworks often focus on developing forward and inverse models using either a global or local approach to capture input-output relationships [3].

Global methods risk overfitting and computational overload, while local methods suffer from limited generalization and hyperparameter sensitivity [9, 10]. Despite advancements in computational power and data availability, deep learning faces challenges due to the neglect of prior principled knowledge, making it difficult to determine dedicated neural network architectures [11, 12].

### 2.1.1 End-to-end learning

#### 2.1.1.1 Classical neural networks model learning

Model-learning problems using neural networks (NN) mainly involves:

1. Input/output data collection: assumed to be available
2. Architecture design: usually found by trial and error
3. Parameter optimization/learning: via well understood schemes, e.g., backpropagation and variants

Designing NN for a particular problem requires experts to determine the best topology, i.e. the number of nodes and layers, connectivity, and activation functions [13]. Furthermore, generalization is difficult as the architecture needs to balance achieving accuracy while avoiding overfitting [13–18]. Therefore, if a NN is used without any model information, large amounts of training data are required to generalize to unknown data [19].

### 2.1.1.2 Topology learning related works

Finding NN topologies is an important and challenging step [11, 14, 20]. Normally, function approximation via NN uses empirical topologies that rely on numerous parameters and do not lend themselves to interpretation. Such models provide no insight into the actual relation between the system variables. Recent works have aimed to find optimal topologies automatically. For example, evolutionary methods have been utilized to optimize the topology of Feed Forward NN (FFNN) [13, 14] as well as deep NN [20], by adding/deleting connections and weights. Constructive methods [16] and pruning methods [21] have also been applied to FFNN. Another method used for FFNN represents the network as a graph and reduces its degrees-of-freedom (DoF) [15]. Furthermore, reinforcement learning (through Q-learning) and topology learning (using variance analysis) have also been implemented to generate architectures [11, 22]. Noticeably, for learning complex dynamical systems, such as articulated robot structures, results have been limited in accuracy and generalization capabilities [3, 23, 24].

### 2.1.1.3 Robot inverse dynamics estimation via classical NN

NN have been applied in numerous variants to model robot inverse dynamics. In [25], Hopfield NN were applied to identify the inertial parameters. Likewise, in [26] a FFNN that used the regressor matrix as training samples was applied. Extreme Learning Machines were utilized in [27] with the same purpose. More recently a two-hidden-layers network with rectified linear activation units (ReLU) was used in [28]. Similarly, recurrent NN have been used to account for the sequential nature of the data. In [29], a recurrent NN in the hidden layer of an otherwise conventional three-layer FFNN was proposed. Additionally, self-organizing networks, in conjunction with echo state networks, were used in [30] via a real-time deep learning algorithm.

## 2.2 Data-driven learning with structure information

In lieu of the challenges faced by deep learning to capture the intricacies of complex systems from scratch, issues such as low sample efficiency, extended training times, and limited generalization highlight the necessity of balancing data-driven and principle-driven approaches [31, 32]. Recently, there has been a growing acknowledgment of the importance of integrating structure into the learning of physical systems [33, 34].

## 2.3 Model learning and the body schema

Building on the significance of structure in model learning for robotics, this dissertation addresses the inference of essential morphological properties in tree-like floating base structures, mimicking the development of a body schema. Efforts in cognitive robotics stress the pivotal role of internal body models in enhancing spatial awareness, motor control, and adaptability [35,36]. However, consensus is lacking on what constitutes a robot’s body schema. Some approaches focus solely on learning the kinematic structure, relying predominantly on off-body vision [37–42]. Others explore sensorimotor associations between proprioceptive, tactile, and visual modalities [43–47], but they provide limited insights into the robot’s physical structure.

Model-based robotics offers reliable methods for identifying physical attributes of robots based on known mechanical topologies. Conventional calibration routines [48] and offline system identification methods [49, 50] are effective for known kinematic structures in controlled environments. However, these methods face challenges when applied to floating base robots without standardized identification procedures [51, 52]. Importantly, these conventional methods were not initially designed for integration into online learning frameworks. While model-based robotics addresses kinematic calibration and forward/inverse kinematics, it provides limited insights into the comprehensive understanding of joint and link arrangement, known as mechanical topology. In cognitive robotics, only a few studies have approached this problem for self-modeling and monitoring, relying on exteroceptive vision [53, 54]. Regardless of the approach taken—black-box machine learning, cognitive methods, or model-based robotics—reliance on external measurement devices persists, overlooking embodied sensing modalities.

In summary, current robotics research reveals gaps in understanding and methods for refining body models. A comprehensive interpretation of the robot body schema and the determination of essential features are crucial. Identifying the fundamental set of necessary signals, both proprioceptive and embodied exteroceptive, is paramount. Integrating advanced machine learning with prior information and first-order principles shows promise for enhanced body models, addressing data requirements and generalization issues. However, the lack of synergy between modeling and learning approaches, along with the absence of a unified scheme for relevant learning stages, represents notable gaps requiring attention to advance robotics into more sophisticated and adaptable embodied systems.

## 2.4 Model learning in robotics

### 2.4.1 Classical and recent works in system identification

### 2.4.2 Local and global models linear models

### 2.4.3 End-to-end learning (black box models)

## 2.5 Data-driven learning with structure information

## 2.6 Model learning and the body schema

### 2.6.1 Internal representations

### 2.6.2 Sensorimotor maps



# 3

## Theoretical Foundations

### 3.1 Introduction

The crucial ability of robots to acquire, refine, and adapt their body models significantly enhances their locomotion, manipulation, and interaction capabilities. However, existing robotics learning frameworks often overlook the robot's physical structure, referred to as its morphology. The concept of the body schema, originating from psychology and neuroscience, is adopted in robotics to represent a model of the robot's morphology. However, current works typically focus on learning kinematic structural properties or exclusively representing sensorimotor associations between proprioceptive, tactile, and visual modalities.

This chapter aims to demonstrate the inherent link between constructing a robot body schema and model-based robotics. Model-based robotics provides established methods for calibrating and identifying physical attributes, albeit under the assumption of a known kinematic structure. In contrast to the online construction and maintenance of the body schema relying on proprioception, these methods were designed for controlled environments, using external devices and offline optimization frameworks.

The chapter commences by introducing the notion of the physical self and related concepts such as embodiment, body morphology, and the body schema. Once these concepts are established, the discussion surveys fundamental bodily features associated with these definitions. Shifting to the realm of robotics, the chapter revisits methods from model-based robotics that offer relevant features for the robotic body schema. It further explores concepts

and methods from complementary disciplines, providing tools to construct a robotic body schema that encompasses a more comprehensive description of the body morphology.

## 3.2 Different views on the body and its features

### 3.2.1 The physical self

The concept of the physical self is rooted in human psychology and consciousness [55, 56]. It typically refers to an individual's perception and evaluation of the physical body, encompassing appearance, abilities, and overall physicality. It involves the subjective experience through diverse sensory modalities (like proprioception and touch) of the body and its relation to the environment. The physical self is directly related to three strongly intertwined concepts: body morphology, embodiment, and body schema—see Fig. 3.1.

In the context of robotics, although robots lack subjective experiences, self-awareness, and consciousness, the physical self remains a critical concept. Robots must perceive their bodies in space to operate effectively in diverse environments. Embodiment in robotics emphasizes how a robot's physical form and sensory-motor capabilities influence its interaction with the environment, shaping its perception and actions within its surroundings [57]. This concept is intrinsically related to the robot morphology, which refers to the physical structure of a robot including its sensors and actuators. In turn, the latter two connect to the notion of body schema, as it represents a model that equips the robot with spatial and inertial awareness of its body.

For a robot, achieving a sense of the physical self requires to leverage its perception and actuation capabilities to acquire knowledge about its bodily attributes through the perceived consequences of its interactions with itself and the environment. This knowledge is encoded in the internal representation of the robot's body.

#### 3.2.1.1 Embodiment

Embodiment, rooted in the hypothesis that intelligence necessitates a body [7, 58], refers to the understanding that a robot's physical body and sensorimotor capabilities shape its interactions within its environment, influencing perception and actions [59, 60]. This involves considerations of the robot's physical structure, situatedness, and morphology, extending beyond functionality to impact interactions with the external world [61]. At the core of embodiment is the body morphology, which significantly influences movement, interaction capabilities, and overall functionality [62]. Embodiment also implies situatedness; that is, robots directly interact with their environment, finding statistical regularities in the sensorimotor experiences [63] and enhancing autonomy and adaptability [64].

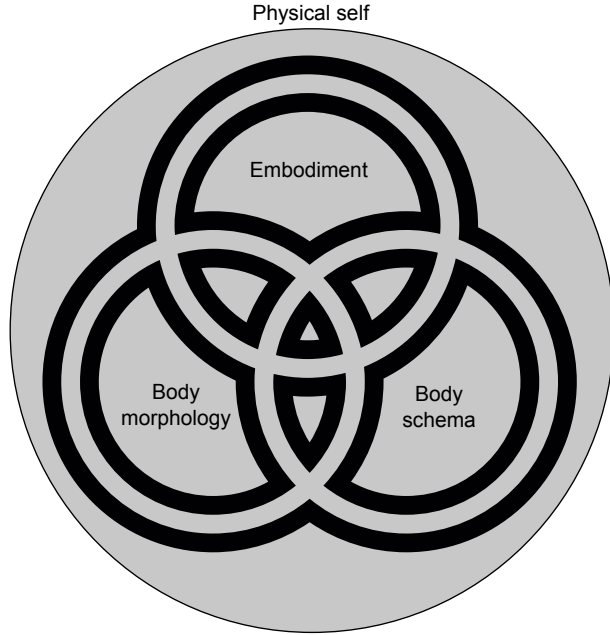


**Figure 3.1: Overlapping concepts.** Embodiment, body morphology, and body schema are three intersection concepts all involved in the definition of the physical self.

### 3.2.1.2 The body morphology

The robot body morphology encompasses its physical structure, including the configuration of joints, limbs, sensors, and actuators [65], playing a pivotal role in determining its capabilities and performance. The joints, serving as points of articulation, allow varied motion, with types like revolute, prismatic, and universal joints offering different degrees of flexibility. Limbs, the appendages extending from the body, consist of links and joints, defining the robot's range of motion and dexterity. Sensors provide information about the environment and internal state, influencing perception and decision-making. Actuators converting energy into mechanical motion and drive joint and limb movement, determining strength and endurance.

### 3.2.1.3 The body schema

Humans rely on a sophisticated internal representation of the body, known as the body schema, to control the body, and interact with the environment. The body schema has been described as consisting of sensorimotor representations guiding actions [66, 67]. Alternatively, it is seen as an internal representations of the body's current posture and spatial extension [68] (including a description of size and shape of different body parts), obtained from tactile, proprioceptive, visual, and other sensory modalities [69]. In essence, the body schema is dynamic representation that encodes several attributes of the body [67, 70, 71]. It is emergent from sensorimotor interactions and yields an enhanced bodily awareness that

Concept	Essence	Relationship
Physical self	Awareness of the body and its interactions with the environment	Overarching concept
Embodiment	The idea that experiences are shaped by the physical body	Foundation for the physical self
Body morphology	The physical structure of the body, including sensorimotor capabilities	Manifestation of embodiment
Body schema	Internal model of the body's physical structure and properties	Dynamic representation of the morphology

Table 3.1: Relationships between the body concepts

allows precise and coordinated movements. The body schema plays an important role in shaping the experience of the physical self, as it is directly involved in the ability to perceive, move, and coordinate the body effectively.

The above description incites the question: *what concretely is the body schema in robotics?* From the various takes on this topic, efforts to consolidate an answer to this question were provided in the comprehensive work by Hoffmann et al. [36]. Relevant to this dissertation is the discussion in [36] about explicit, articulated, and implicit models of the body schema. The first two categories correspond to models where there is a direct correspondence between the body parts of the robot and their representation in the model, given measurements from variables that can be associated to properties of the physical body. The main difference being that articulated models [72] emphasize that the signals ought to come from embodied sensors. This latter property has been referred as subjective or situated body schema [37]. The third category, implicit body schema, is more inline with traditional model learning methods in robotics and is aimed at constructing sensorimotor mappings.

### 3.2.2 Summary of the body concepts

The physical self, embodiment, body morphology, and body schema are interconnected concepts crucial for understanding bodily awareness. The physical self is an overarching concept that involves awareness and perception of the body and its movements. Embodiment posits that experiences are shaped by the physical body, influencing the self-constructed representations of the body and environment. Body morphology, is the specific instantiation of embodiment encompassing body structural description and sensorimotor properties. The body schema is the adaptable representation of the morphology based on sensorimotor interaction. Table 3.1 condenses the essence and relationships of these body con-

cepts. As will be shown in the subsequent discussion, the body schema in robotics is the entry points for robots to acquire an understanding of their physical self.

### 3.3 The robot body schema

Embodiment and robot morphology are almost equivalent concepts that relate to the actual physical attributes of the robot body. As accentuated by the rich literature in model-based robotics, models of robots that capture these attributes are required to achieve fine control and perform complex tasks. These models should include as much information as possible, explicit or implicit, of their embodiment. A body schema is a model that serves this purpose. Most of the efforts associated with learning the body schema agree on the argument that an embodied robotic agent must autonomously learn and refine its body schema relying mainly proprioceptive information [36, 71]. Yet, in spite of the many bodily features encoded in the body schema, the majority of research focus on calibration of a known kinematic structure [37, 73, 74] and only a few works address the discovery of the body topology [54]. Additionally, **it is worth mentioning that there is no solid consensus in the literature about whether the body schema includes the inertial description of the parts composing the body. Yet, given that the body schema is used for planning and executing movements and that the sensation of effort (force and torque) is part of proprioception, it seems reasonable to assume the body schema could incorporate such a representation.** Ultimately, the question remains of what constitutes a body schema in robotics.

To continue the discussion in this work the following conceptual definition of the robot body schema will be used:

**Definition 3.1.** The robot body schema is a representation of its body morphology primarily constructed from proprioceptive information. This representation encompasses the arrangement, geometry, and inertial properties of its body parts, providing the capacity to perceive their state of motion and to plan and execute movements independent from visual inputs. Adaptive and self-acquired, the robot body schema plays a fundamental role in forward and inverse models, aiding in the integration, planning and prediction of sensorimotor interactions beyond proprioception.

#### 3.3.1 Properties of the body schema

This section provides an overview of some of the most relevant attributes from the body morphology encoded by the body schema (see Fig. 3.2).

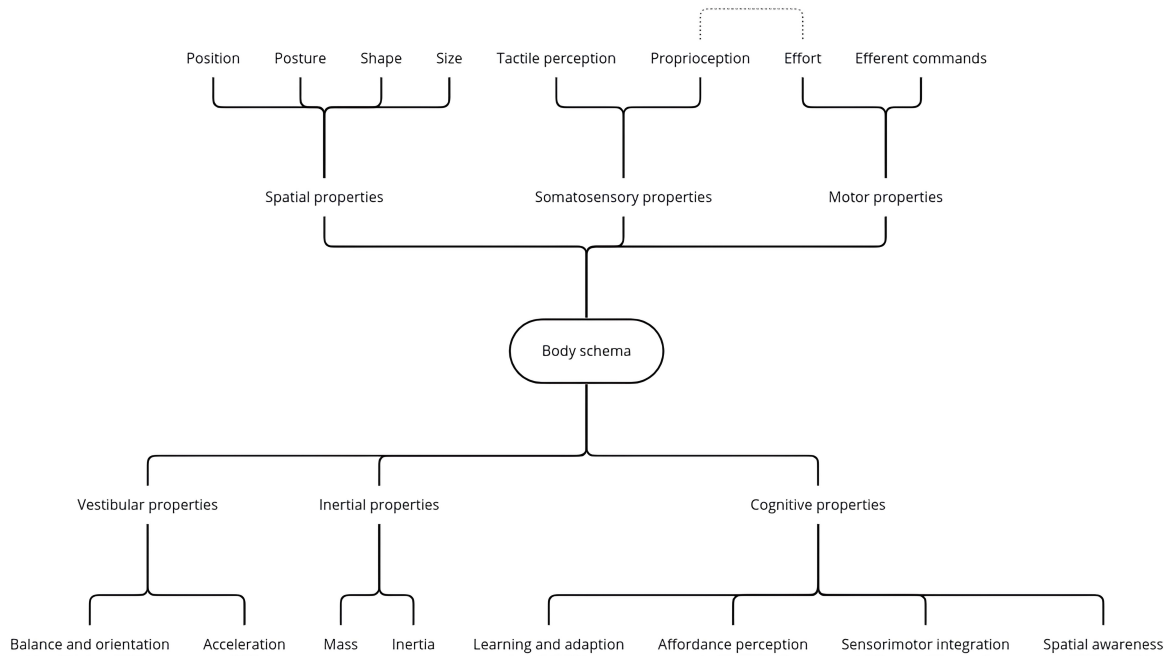


**Figure 3.2: Properties of the body schema.** The body schema subsumes several properties of the body morphology.

**Spatial properties** The body schema includes a representation of the size and shape of different body parts. Additionally, information about their spatial orientation and position in relation to each other is part of the schema. This is essential for accurate and coordinated movements and interactions.

**Somatosensory properties** The two main sensory modalities in somatosensation are proprioception and touch [75]. The former is the sense of position, movement, and effort of the body parts. The latter, conveys information about pressure and temperature that complement the body description and can be used to form a three-dimensional interpretation of the body.

**Vestibular properties** Vestibular signals play a critical role in maintaining balance. These signals offer vital information about the body's orientation in space, encompassing both linear and angular motion states. Whether engaged in locomotion, manipulation, or adjusting posture, vestibular signals seamlessly collaborate with proprioception to shape the body schema.

**Inertial properties** The inertial description of the body encompass characteristics associated with the mass distribution of the body parts. This knowledge holds crucial significance for both forward and inverse models in motor control. In the process of planning a movement, the inertial properties of the body schema come into play as they are utilized to es-

timate the forces and torques necessary for moving various body parts. Subsequently, this information is employed to generate motor commands.

**Cognitive properties** The body schema enables the understanding of the morphological properties of the body and improves the formation of regularities between perception and action by integrating multimodal sensory inputs. It also helps perceive the affordances of objects and of the body itself. Furthermore, the body schema's plasticity allows constant updates, incorporating information from novel movements, environmental interactions, and changes in the body for improved motor performance and adaptation.

**Motor Properties** The body schema is closely tied to motor control and the execution of movement. As mentioned before, it is an essential component of forward and inverse models used to generate and predict the consequences of motor commands.

## 3.4 Robotics and the properties of the body schema

In the coming discussion an overview of the tools and methods from robotics and other disciplines that either are or can be used to represent some of the properties of the body schema presented in Sec. 3.3.1 is provided.

### 3.4.1 Perceiving the body: Robot proprioception

Proprioception, encompassing the awareness of body position, movement, and effort, plays a crucial role in executing coordinated movements [77, 78]. In humans, mechanoreceptors such as muscle spindles and Golgi tendon organs, embedded in joints, muscles, and tendons, provide proprioceptive information, detecting features like joint position, movement, and effort [78]. These signals are transmitted to the central nervous system, where they integrate with information from other sensory systems, including visual and vestibular, to form an overall representation of the body's state. Proprioception is commonly divided into two sub-modalities: kinaesthesia, associated with the sense of limb movement, and joint position sense, linked to the sense of limb position [79, 80]. Additionally, a third sub-modality, sometimes considered separately, is effort, which involves the perception of tension, force, and heaviness related to motor commands [78]. Proprioception is fundamental to the body schema, as it contributes to its formation and ensures its adaptability [81].

Similar to how humans rely on proprioception to be aware of their body's position and movement, robots leverage proprioceptive capabilities to understand their own kinematics and dynamics. This information is crucial for robots to execute precise and coordinated

movements, adapt to changes in their environment, and interact effectively. Some relevant proprioceptive sensors in robotics include [82]:

- **Joint encoders:** Provide feedback on the angular displacement of the joints, allowing the robot to determine its joint angles accurately. Conventionally, numerical differentiation of these signals are used to convey joint velocity.
- **Gyroscopes:** Measure the angular velocity of a body. They help in determining the orientation and changes in orientation over time of the robot body parts. Gyroscopic sensors contribute to maintaining stability and control in dynamic motions.
- **Accelerometers:** Monitor the linear acceleration of a body in various directions. Accelerometers are vital for tasks requiring dynamic motion analysis.
- **Strain gauges:** Strain gauges are used mostly in robot joints to provide feedback on the torque. They are used for torque controlled robots and are fundamental in collision detection frameworks.
- **Force/Torque sensors:** Measure the wrench applied to a robot's end-effector or joints. The feedback provided by these sensors enable it to perceive its own body, and to respond and adapt to interactions with objects or the environment.

### 3.4.2 Modeling body size, position, and posture: Robot kinematics

A serial kinematic chain is a sequence of rigid bodies called links connected by joints. In a serial kinematic chain the output of one joint becomes the input for the next and there are no loops. Robots, such as manipulators, legged robots, and humanoids, are instances of serial kinematic chains. The motion of the robot is achieved by the controlled rotation or translation of each joint. A robot is said to be of fixed base if the first link in the chain (base link) is rigidly connected to the world. The best example being robot manipulators. On the contrary, in floating base robots, the base and all other links can freely rotate and translate in space. Humanoid robots are a good example of this type. The focus in this work is on serial kinematic chains with either fixed or floating bases and revolute joints.

Robot joints can be classified into various types. One degree of freedom (DOF) joints include revolute joints (rotational motion about the joint axis), prismatic joints (translational motion along the direction of the joint axis), and helical joints (simultaneous rotation and translation about a screw axis) [83]. Joints can also have multiple degrees of freedom allowing independent translations and rotations about multiple axes. The configuration and number of joints in the chain determine the robot's total DOF. Typically a joint variable  $q$  is used to express the translational or angular displacement between the links connected by a

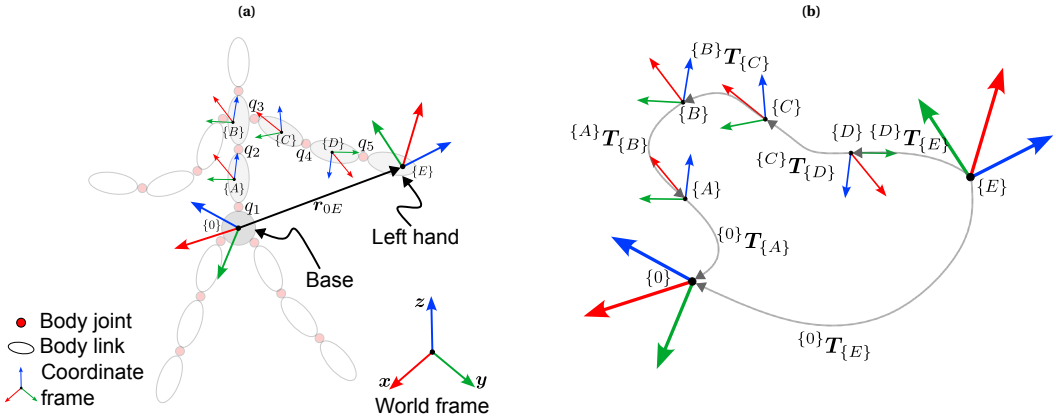


**Figure 3.3: A serial kinematic chain and its transformations.** (a) A humanoid is a serial kinematic chain with a floating base. Two coordinate frames are shown, one at the base and one at the left hand link. (b) The sequence of coordinate transformations from frame  $\{0\}$  to  $\{E\}$ .

one-DOF joint. For a robot with  $n$  joints, the configuration is described by the vector

$$\mathbf{q} = [q_1, \dots, q_i, \dots, q_n]^\top \in \mathbb{R}^n. \quad (3.1)$$

Joint axes are modeled as lines in space, represented as a vector, that indicate the direction about which a joint rotates or translates. In general, the range of mobility  $[a, b]$  of a joint is mechanically constrained by upper  $a$  and lower  $b$  limits. The Cartesian product of all joint ranges is the configuration space of the robot [83].

The pose of a rigid body in the kinematic chain represents the position and orientation of a coordinate frame rigidly attached to it with respect to a reference frame [85]. A minimum of six parameters is needed to completely instantiate pose of a rigid body in Euclidean space [83]. The pose of a given body is dependent on all the joint variables from the base to the current joint as well as on the geometry of the links. Considering the simplified humanoid robot shown in Fig. 3.3a as an example, the link corresponding to the left hand has the frame  $\{E\}$  rigidly attached to it. Its pose can be expressed relative to the coordinate frame  $\{0\}$  located at the humanoid's base link via the homogeneous transformation matrix

$$\{0\}T_{\{E\}} = \begin{bmatrix} \{0\}R_{\{E\}}(\mathbf{q}) & \{0\}r_{0E}(\mathbf{q}) \\ 0_{1 \times 3} & 1 \end{bmatrix} \in \mathbb{R}^{4 \times 4}. \quad (3.2)$$

The vector  $\{0\}r_{0E}(\mathbf{q}) \in \mathbb{R}^3$  denotes the location of the origin of the coordinate frame  $\{E\}$  relative to and expressed in frame  $\{0\}$ . Similarly, the rotation matrix  $\{0\}R_{\{E\}}(\mathbf{q}) \in \mathbb{R}^{3 \times 3}$  expresses the orientation of frame  $\{E\}$  in frame  $\{0\}$ . Both terms are function of the robot configuration vector  $\mathbf{q}$ .

A rotation matrix is orthogonal, that is  $R^{-1} = R^\top$ , and has unit determinant. Any rotation matrix belongs to the set of all rotation matrices, which is a group known as the rotation

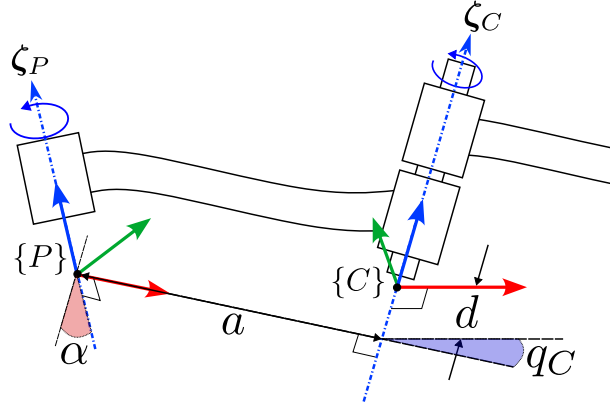


**Figure 3.4: MDH frame convention.** The location and orientation of the joint frames in the MDH convention depends on three fixed parameters  $(a, \alpha, d)$  and the joint angle  $q_C$ .

group or the special orthogonal group  $\text{SO}(3)$  [83]. A composition of rotations is achieved by the matrix product of two or more rotation matrices. Similarly, the set of all transformation matrices defines the special Euclidean group  $\text{SE}(3)$ , which represents the group of rigid body motions in 3D space. Just like rotation matrices, all the elements of  $\text{SE}(3)$  are orthogonal and have determinant equal to 1. Referring back to Fig. 3.3a, the composition of transformation matrices from the left hand of the humanoid to its base yields the following expression

$$\{^0\}\mathbf{T}_{\{E\}} = \{^0\}\mathbf{T}_{\{A\}}(q_1) \{^A\}\mathbf{T}_{\{B\}}(q_2) \{^B\}\mathbf{T}_{\{C\}}(q_3) \{^C\}\mathbf{T}_{\{D\}}(q_4) \{^D\}\mathbf{T}_{\{E\}}(q_5), \quad (3.3)$$

a graphical depiction of this sequence of transformations is shown in Fig. 3.3b.

In general, describing the kinematic structure of a robot consists in expressing the location and orientation of the frames attached to the composing links. This is conventionally achieved by associating a homogeneous transformation matrix to each of the  $n+1$  rigid bodies in the kinematic chain.

### 3.4.2.1 Representation of transformation matrices

**Modified Denavit-Hartenberg representation** The modified Denavit-Hartenberg (MDH) convention uses four unique parameters per link to describe the kinematics of robots. With reference to Fig. 3.4, the MDH parameters represent the link length  $a$  (the offset distance between the joint axes  $\zeta_P$  and  $\zeta_C$ ), the link twist  $\alpha$ , the link offset  $d$ , and the joint angle  $q_C$ . The set of MDH parameters  $(a, \alpha, d, q_C)$  describe the location and orientation of the joint frames in a robot [86]. The MDH parameters of a joint are used to define the parameter

vector  $\lambda^{DH} = [\lambda_1, \lambda_2, \lambda_3, \lambda_4]^\top$  and build with it the following transformation matrix:

$$\{P\}\mathbf{T}_{\{C\}} = \begin{bmatrix} \cos(q_C) & -\sin(q_C) & 0 & \lambda_1 \\ \sin(q_C)\lambda_3 & \cos(q_C)\lambda_3 & -\lambda_2 & -\lambda_2\lambda_4 \\ \sin(q_C)\lambda_2 & \cos(q_C)\lambda_2 & \lambda_3 & \lambda_3\lambda_4 \\ 0 & 0 & 0 & 1 \end{bmatrix}, \quad (3.4)$$

with  $\lambda_1 = a$ ,  $\lambda_2 = \sin(\alpha)$ ,  $\lambda_3 = \cos(\alpha)$ , and  $\lambda_4 = d$ .

**Euler angles representation** A vector  $\lambda^{EA} = [\lambda_1, \lambda_2, \lambda_3, \lambda_4, \lambda_5, \lambda_6]^\top$  is used to define a homogeneous transformation matrix based on a rotation matrix

$$\{C\}\mathbf{R}_{\{P\}} = (\text{Rot}_z(\lambda_1)\text{Rot}_x(\lambda_2)\text{Rot}_z(\lambda_3)\text{Rot}_z(q_C))^\top \quad (3.5)$$

depending on the Euler angles [85]  $(\lambda_1, \lambda_2, \lambda_3)$  and the translation vector  $\{P\}\mathbf{r}_{\{C\}} = [\lambda_4, \lambda_5, \lambda_6]^\top$ . The expression  $\text{Rot}_i(j)$  defines a pure rotation of  $j$  radians around the axis  $i$ .

**Axis-angle representation** A vector of parameters

$$\lambda^{AA} = \left[ \{P\}\boldsymbol{\xi}_C^\top \quad \phi \quad \{C\}\boldsymbol{\zeta}_C^\top \quad \{P\}\mathbf{r}_C^\top \right]^\top \in \mathbb{R}^{10} \quad (3.6)$$

determines the rotation matrix  $\{P\}\mathbf{R}_{\{C\}}^T$  in axis-angle form [83] as

$$\{P\}\mathbf{R}_{\{C\}}(q_C; \gamma) = \left( \exp^{[\{P\}\boldsymbol{\xi}_C]\phi} \right) \left( \exp^{[\{C\}\boldsymbol{\zeta}_C]q_C} \right). \quad (3.7)$$

The terms  $\boldsymbol{\xi} \in \mathbb{R}^3$  and  $\boldsymbol{\zeta} \in \mathbb{R}^3$  are unitary rotation axes and  $[\cdot]$  denotes a vector  $\mathbf{u} = [u_x, u_y, u_z]^\top$  expressed as a skew-symmetric matrix; i.e.,

$$[\mathbf{u}] = \begin{bmatrix} 0 & -u_z & u_y \\ u_z & 0 & -u_x \\ -u_y & u_x & 0 \end{bmatrix}. \quad (3.8)$$

The vector  $\boldsymbol{\zeta}$  expresses the rotation axis of the joint that connects two bodies, expressed in the coordinate system  $\{C\}$  of the child body. The angle  $\phi$  defines the constant rotation about the axis  $\boldsymbol{\xi}$  defined by the geometry of the links alone when the joint angle  $q_C$  is zero.

### 3.4.2.2 Forward differential kinematics

The motion of a rigid body in a kinematic chain is a composition of pure translation and rotation. The twist vector  $\boldsymbol{\nu} \in \mathbb{R}^6$  contains the Cartesian linear (translational) velocity  $\mathbf{v} \in \mathbb{R}^3$

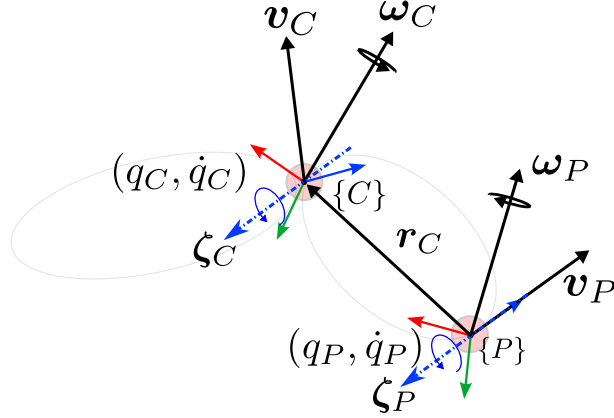


**Figure 3.5: Body twist.** A twist is composed of the linear and angular velocities at a point on a rigid body.

and the Cartesian angular velocity  $\omega \in \mathbb{R}^3$  of a point in the body; i.e.,

$$\nu = [v^\top, \omega^\top]^\top.$$

The twist of a child body  $C$  depends on the position  $q_C$  and velocity  $\dot{q}_C$  of its driving joint, the twist of the parent link  $P$  ( $v_P, \omega_P$ ), and the geometry of the links. The corresponding expressions are

$$\{C\}v_C = \{C\} R_{\{P\}}(q_C) (\{P\}v_P + [\{P\}\omega_p] \{C\}r_C) \quad (3.9)$$

for the linear velocity and

$$\{C\}\omega_C = \{C\} R_{\{P\}}(q_C) (\{P\}\omega_P + \dot{q}_C \{C\}\zeta_C) \quad (3.10)$$

for the angular velocity [87]. The term  $\{C\}\zeta_C \in \mathbb{R}^3$  in Eq. (3.10) is the unit vector that represents the joint rotation axis of the child joint. These quantities are depicted in Fig. 3.5. The time derivative of the twist vector gives the linear and angular acceleration of the rigid body [85]; i.e.,

$$\{C\}\dot{v}_C = \{C\} R_{\{P\}}(q_C) (\{P\}\dot{v}_P + ([\{P\}\omega_P] [\{P\}\omega_P] + [\{P\}\dot{\omega}_P]) \{P\}r_C) \quad (3.11)$$

and

$$\{C\}\dot{\omega}_C = \{C\} R_{\{P\}}(q_C) (\{P\}\dot{\omega}_P + \ddot{q}_C \{C\}\zeta_C + \dot{q}_C [\{P\}\omega_P] \{C\}\zeta_C). \quad (3.12)$$

### 3.4.2.3 Kinematic calibration

Kinematic calibration is crucial for robotic systems, particularly for floating base multi limb kinematic structures. It involves enhancing the accuracy of a robot's positioning by adjusting its kinematics control model, all without making any alterations to its hardware [88]. Accurate calibration ensures robots can perform tasks with precision and safety. Various online and offline methods have been developed, requiring a reference measurement system and

involving modeling, measurement, and optimization of kinematic parameters [89].

Two primary approaches have been developed for kinematic calibration: model-based and non-parametric (model-less) calibration [88]. Model-based calibration utilizes a mathematical model of the robot's kinematic structure, typically represented by the DH parameters. The calibration process involves measuring joint angles and end-effector poses for various configurations and then estimating the DH parameters that best fit the observed data. Model-based calibration offers high accuracy but is sensitive to errors in the robot's model. Model-less calibration, on the other hand, does not rely on a predefined kinematic model. Instead, it estimates the relationship between joint angles and end-effector pose using a set of external markers, fiducial markers, or visual features in the robot's environment. Model-less calibration is more robust to model inaccuracies but can be more computationally demanding and complex.

Calibrating floating base systems, like humanoid and legged robots, is challenging due to their complex kinematic structure, geometrical uncertainties, sensor noise, and dynamic environment [REF](#). The hierarchical tree structure with multiple joints and links makes accurate calibration computationally challenging. Geometrical uncertainties from manufacturing tolerances, wear and environmental factors can introduce errors, affecting the accuracy of the estimated kinematic parameters. Sensor noise, from on-board and off-board measurement devices, adds uncertainty, impacting parameter accuracy, particularly in dynamic environments. The dynamic nature of these robots, with rapidly changing movements and environmental conditions, further complicates calibration, which requires continuous adaptation and monitoring.

**Calibration methods** Various methods are used to perform kinematic calibration, each with its own advantages and limitations.

- Marker-based calibration. This method relies on external markers at a location  $x_i$  attached to the robot's body. A camera system tracks the movements of these markers, and the calibration process estimates the relationship between the measured joint angles  $q$  and marker positions. This makes use of the robot forward kinematics formulation

$$x_i = f(q; \lambda), \quad (3.13)$$

relying on an initial (uncalibrated) estimate  $\lambda_0$ . This method is relatively accurate and can handle complex kinematic structures. However, it requires careful marker placement and is sensitive to marker occlusion.

- Laser tracker-based calibration. Uses a laser tracker to measure the position and orientation of the robot's end-effector in space. The calibration process estimates the relationship between joint angles and end-effector pose based on these measurements.

This method is highly accurate, especially for robots with large workspaces. However, it is more expensive and requires a dedicated laser tracker system.

- Vision-based calibration. It utilizes a camera system to observe the robot's movements and identify reference points or features in the environment. The calibration process estimates the relationship between joint angles and reference points based on these observations. This method can be used in unstructured environments; however, it can be sensitive to lighting conditions, camera calibration errors, and the difficulty of identifying suitable reference points.
- IMU-based calibration. The process uses inertial measurement units (IMUs) to measure the robot's orientation and angular velocity and estimates the relationship between joint angles and IMU measurements based on the robot's known initial pose and orientation. This method can be used in real-time, but it is not as accurate as marker-based or laser tracker-based calibration, and it can be affected by sensor noise and drift.

It is worth noting that calibration of robots has been conventionally performed in controlled environments relying mostly on external metrology devices. Current research explores methods and techniques to address the challenges of kinematic calibration of floating base robots. The ultimate goal is to achieve self-calibration by relying on on-board sensors and algorithms, thus eliminating the need for external measurements and reference points. Adaptive calibration should also be a part of this process to monitor the structure, consider potential changes, and adjust kinematic parameters or descriptions in real-time. Online calibration enables robots to calibrate themselves during operation, eliminating the need to pause or move to specific locations.

### 3.4.3 The inertial properties of the body schema

The dynamic parameters of the  $i$ -th rigid body in a kinematic chain include its mass  $m_i$ , the center of mass  $\mathbf{C}_i = [X_i, Y_i, Z_i]^\top$ , and inertia matrix  $\mathbf{I}_i$ . The latter is dependent on the reference frame in which it is expressed. The inertia matrix  $\mathbf{I}_i \in \mathbb{R}^{3 \times 3}$  of the  $i$ -th link defined in the coordinate frame of the  $i$ -th joint is given by:

$$\mathbf{I}_i = \mathbf{I}_i^\top = \begin{bmatrix} XX_i & XY_i & XZ_i \\ XY_i & YY_i & YZ_i \\ XZ_i & YZ_i & ZZ_i \end{bmatrix}, \quad (3.14)$$

where the elements of the triplet  $(XX_i, YY_i, ZZ_i)$  represent the moments of inertia and the terms  $(XY_i, XZ_i, YZ_i)$  are the products of inertia. They can be summarized in the vector of

inertial parameters

$$\boldsymbol{\theta}_i = \begin{bmatrix} m_i & \mathbf{mC}_i & XX_i & XY_i & XZ_i & YY_i & YZ_i & ZZ_i \end{bmatrix}^\top \in \mathbb{R}^{10}. \quad (3.15)$$

The term  $\mathbf{mC}$  is the first moment of mass vector defined as

$$\mathbf{mC}_i = \begin{bmatrix} m_i X_i & m_i Y_i & m_i Z_i \end{bmatrix}^\top, \quad (3.16)$$

which is the product of the link mass and its center of mass vector.

The inertial parameters  $\boldsymbol{\theta}_i$  are related to the motion of link  $i$  by the Newton-Euler equations [90]:

$$\underbrace{\begin{bmatrix} \{i\} \mathbf{f}_{ii} \\ \{i\} \mathbf{n}_{ii} \end{bmatrix}}_{\mathbf{w}_{ii}} = \underbrace{\begin{bmatrix} (\{i\} \dot{\mathbf{v}}_i - \mathbf{g}) & [\{i\} \dot{\omega}_i] + [\{i\} \omega_i] [\{i\} \omega_i] \\ \mathbf{0}_{3 \times 1} & [(\mathbf{g} - \{i\} \dot{\mathbf{v}}_i)] \end{bmatrix}}_{\mathbf{A}_i} \underbrace{\begin{bmatrix} \mathbf{0}_{3 \times 6} \\ [\bullet \{i\} \dot{\omega}_i] + [\{i\} \omega_i] [\bullet \{i\} \omega_i] \end{bmatrix}}_{\boldsymbol{\theta}_i}, \quad (3.17)$$

where the wrench  $\mathbf{w}_{ii} = [\mathbf{f}_{ii}^\top, \mathbf{n}_{ii}^\top]^\top$  corresponds to the force and moment at joint  $i$  due to the inertial properties of link  $i$  only. The term  $\mathbf{g} = [0, 0, -9.81]^\top$  m/s is the gravitational acceleration vector and the Cartesian linear and angular accelerations are expressed according to Eq. (3.11) and Eq. (3.12). The term  $[\bullet \omega_i]$  is defined as

$$[\bullet \omega] = \begin{bmatrix} \omega_x & \omega_y & \omega_z & 0 & 0 & 0 \\ 0 & \omega_x & 0 & \omega_y & \omega_z & 0 \\ 0 & 0 & \omega_x & 0 & \omega_y & \omega_z \end{bmatrix}. \quad (3.18)$$

As a result of joint  $j$  exerting a wrench on its associated link  $j$ , there will be a reacting wrench onto link  $i$ ; as such,  $\{i\} \mathbf{w}_{ij} \in \mathbb{R}^6$  is the wrench at joint  $i$  due to the movement of link  $j$  alone. Given a transformation matrix  $\{i\} \mathbf{T}_{\{j\}}$  defined by a tuple  $(\{i\} \mathbf{R}_{\{j\}}, \{i\} \mathbf{p}_{\{j\}})$ , its adjoint representation [83]

$$[\text{Ad}_{\mathbf{T}_j}] = \begin{bmatrix} \{i\} \mathbf{R}_{\{j\}} & \mathbf{0}_{3 \times 3} \\ [\{i\} \mathbf{p}_j] \{i\} \mathbf{R}_{\{j\}} & \{i\} \mathbf{R}_{\{j\}} \end{bmatrix} \quad (3.19)$$

is understood as a wrench transmission matrix. With it  $\{i\} \mathbf{w}_{ij}$  can be computed as

$$\{i\} \mathbf{w}_{i,j} = [\text{Ad}_{\mathbf{T}_j}] \{j\} \mathbf{w}_{j,j}. \quad (3.20)$$

The effect of all the distal wrenches to a joint  $i$  can be aggregated via the matrix product of the corresponding adjoint operators. For example, the effect of wrench  $\mathbf{w}_{k,k}$  in Fig. 3.6 is

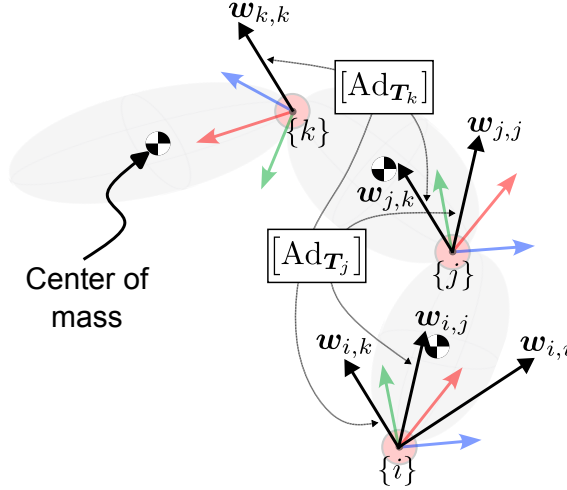


**Figure 3.6: Wrench transmission.** Using the adjoint operator the wrenches at distal joints can be propagated backwards to proximal joints.

propagated to joint  $j$  as

$$\mathbf{w}_{i,k} = \underbrace{\left[ \text{Ad}_{\mathbf{T}_j} \right] \left[ \text{Ad}_{\mathbf{T}_k} \right]}_{U_{i,k}} \mathbf{w}_{k,k} = \left[ \text{Ad}_{\mathbf{T}_j} \right] \left[ \text{Ad}_{\mathbf{T}_k} \right] \overbrace{\mathbf{A}_{k,k}}^{U_{k,k}} \boldsymbol{\theta}_k. \quad (3.21)$$

Finally, the total wrench

$$\mathbf{w}_j = \mathbf{w}_{jj} + \sum_{k=j+1}^N \mathbf{w}_{jk} \quad (3.22)$$

at each of the joints can be expressed in matrix form

$$\begin{bmatrix} \mathbf{w}_i \\ \mathbf{w}_j \\ \vdots \\ \mathbf{w}_n \end{bmatrix} = \begin{bmatrix} U_{i,i} & U_{i,j} & \cdots & U_{i,n} \\ 0 & U_{j,j} & \cdots & U_{j,n} \\ \vdots & \vdots & \ddots & \vdots \\ 0 & 0 & \cdots & U_{n,n} \end{bmatrix} \begin{bmatrix} \boldsymbol{\theta}_i \\ \boldsymbol{\theta}_j \\ \vdots \\ \boldsymbol{\theta}_n \end{bmatrix}. \quad (3.23)$$

This expression corresponds to the inverse dynamics of the robot, that is, its output gives the  $n$  wrench vectors necessary to produce the rigid body motions captured by the quantities  $\{\dot{i}\}\omega_i$ ,  $\{\dot{i}\}\dot{\omega}_i$ , and  $\{\dot{i}\}\dot{v}_i$  for each of the  $n$  joints. Since, typically, only joint torque  $\tau$  is measured, Eq. (3.23) is projected onto the rotation axes of the joints [91] yielding

$$\boldsymbol{\tau} = \mathbf{Y}(\boldsymbol{\omega}, \dot{\boldsymbol{\omega}}, \dot{\boldsymbol{v}}; \boldsymbol{\lambda}) \boldsymbol{\theta} = \mathbf{Y}(q, \dot{q}, \ddot{q}; \boldsymbol{\lambda}) \boldsymbol{\theta}. \quad (3.24)$$

This expression for the inverse dynamics is linear in the parameters (LIP)  $\boldsymbol{\theta}$ . The regressor matrix  $\mathbf{Y}(\cdot)$  is dependent exclusively on the motion of the robot and its geometry  $\boldsymbol{\lambda}$ . The

vector  $\boldsymbol{\theta} \in \mathbb{R}^{10n}$  contains the stacked inertial parameters  $\{\boldsymbol{\theta}_i\}_{i=1}^n$ . The expression in Eq. (3.24) is equivalent to

$$\boldsymbol{\tau} = \mathbf{M}(\boldsymbol{q}; \boldsymbol{\theta}) \ddot{\boldsymbol{q}} + \mathbf{c}(\boldsymbol{q}, \dot{\boldsymbol{q}}; \boldsymbol{\theta}) + \mathbf{g}(\boldsymbol{q}; \boldsymbol{\theta}), \quad (3.25)$$

where  $\mathbf{M}(\cdot)$  is the configuration-dependent mass matrix of the robot,  $\mathbf{c}(\cdot)$  is the vector of centrifugal and Coriolis torques, and  $\mathbf{g}(\cdot)$  is the gravitational torque.

### 3.4.3.1 Estimation of the inertial parameters

**Fixed base** The state of maturity of the research on inertial parameter identification for fixed base robots has lead to a rather standard procedure [49]. Concretely, the process involves the generation of an excitation trajectory [92, 93] —according to some observability index REF—to collect  $P$  measurement points  $(\boldsymbol{\tau}(k), \boldsymbol{q}(k), \dot{\boldsymbol{q}}(k), \ddot{\boldsymbol{q}}(k))$  representing instances of Eq. (3.24). The estimation of the vector of inertial parameters  $\boldsymbol{\theta}$  consists in using this set of points to solve the linear problem

$$\boldsymbol{y} = \mathbf{F}\boldsymbol{\theta}, \quad (3.26)$$

where  $\boldsymbol{y} = [\boldsymbol{\tau}^\top(1), \dots, \boldsymbol{\tau}^\top(k), \dots, \boldsymbol{\tau}^\top(P)]^\top \in \mathbb{R}^{nP}$  and  $\mathbf{F} = [\mathbf{Y}_1^\top, \dots, \mathbf{Y}_k^\top, \dots, \mathbf{Y}_P^\top]^\top \in \mathbb{R}^{nP \times 10n}$ . It is standard to follow a least-squares approach for the estimation of an optimal  $\boldsymbol{\theta}$ ; i.e.

$$\boldsymbol{\theta} = (\mathbf{F}^\top \mathbf{F})^{-1} \mathbf{F}^\top \boldsymbol{y}. \quad (3.27)$$

Methods to address the identifiability, numerical stability, and observability of the parameters have been discussed [91]. For fixed base robots, specifically, it is known that some of the parameters of the links proximal to the base cannot be identified and methods to determine the base set of parameters have been developed [94].

**Floating base** Research in robotics is actively exploring methods for estimating the inertial parameters of floating base systems; in particular, humanoid and legged robots. For instance, there are methods utilizing base-link dynamics, which require generalized coordinates of the base-link, joint angles, and external forces [95–98]. The work by Jovic et al. [99] introduced a hierarchical optimization approach, accurately reconstructing ground reaction forces and force moments. Mistry et al. [100] proposed a method for whole-body inertial parameter estimation, demonstrating feasibility for floating-base humanoid systems using a partial force sensor set. Another state-estimation technique for legged robots, combining forward kinematics and preintegrated contact factors, was introduced by Hartley et al. [101]. Addressing the dynamics of legged systems, Ayusawa et al. [51] proposed a method based on underactuated base-link dynamics for identifying inertial parameters. Buchanan et al. [102] introduced a proprioceptive state estimator for legged robots based on learned displacement measurement from IMU data, significantly reducing drift in challenging scenarios.

Extensions for floating-base robots with flexible joints and links have been presented elsewhere [103]. From the variety of methods, a reasonable conclusion is that, unlike the methods for the inertial parameter estimation of fixed based robots, the methods for floating base robots are not as standardized.

### 3.4.3.2 Physical feasibility of the inertial parameters

More recently, the physical feasibility of the identified parameters has taken a prominent role [104–107]. This is vital due to its importance in ensuring stable control methods. For instance, physically feasible inertial parameters lead to always invertible symmetric positive definite mass matrices. For the inertial parameters of a rigid body to be physically feasible, it is required that its mass is strictly positive and that its inertia matrix  $\mathbf{I}_i$  is symmetric positive definite (SPD) with its eigenvalues — $\mathbf{s}(\mathbf{I}_i) = [s_1, s_2, s_3]^T$ — satisfying the triangle inequality, i.e.:

$$m_i > 0, \quad \mathbf{I}_i > 0, \quad \begin{cases} s_1 + s_2 \geq s_3 \\ s_2 + s_3 \geq s_1 \\ s_1 + s_3 \geq s_2 \end{cases}. \quad (3.28)$$

These physical feasibility constraints can be expressed in the language of differential geometry. To that end, it is first necessary to define a differentiable manifold  $\mathcal{M}$ . It is a topological space that exhibits local similarity to Euclidean space and possesses a globally defined differential structure [108]. At any point  $\mathbf{P}$  on the manifold there is an associated tangent space, denoted as  $\mathcal{T}_{\mathbf{P}}\mathcal{M}$ , that encompasses the vector space containing all possible tangent vectors to  $\mathcal{M}$  that pass through  $\mathbf{P}$ . A Riemannian manifold is defined by the pair  $(\mathcal{M}, \rho)$ , where each point  $\mathbf{P}$  in  $\mathcal{M}$  is equipped with a positive definite metric tensor  $\rho$  [109].

The inertial parameters of rigid body, and by extension of a robot, are associated to the manifolds of SPD matrices. To make clear this relation, let  $\mathcal{S}^n$  be the space of real square symmetric matrices with dimension  $n \times n$ , denoted as  $\mathcal{S}^n \triangleq \{\mathbf{S} \in \mathbb{R}^{n \times n} : \mathbf{S} = \mathbf{S}^T\}$ . The space of  $n \times n$  SPD matrices,  $\mathcal{S}_{++}^n \triangleq \{\mathbf{P} \in \mathcal{S}^n : \mathbf{P} > 0\}$ , defines a smooth submanifold  $\mathcal{M}$  within  $\mathcal{S}^n$ . Its tangent space  $\mathcal{T}\mathcal{M} \in \mathcal{S}^n$  is equipped with an affine invariant Riemannian metric  $\rho$  [110], thereby making  $\mathcal{S}_{++}^n$  a Riemannian manifold. Finally, the Cartesian product  $\mathcal{M}^N = \mathcal{M}_1 \times \mathcal{M}_2 \times \dots \times \mathcal{M}_N$  defines the product manifold of SPD manifolds. It represents the set of matrices  $\{(\mathbf{P}_1, \dots, \mathbf{P}_N) : \mathbf{P}_i \in \mathcal{M}_i, \quad i = 1, \dots, N\}$  and is also a Riemannian manifold with the metric  $\rho = \text{diag}(\rho_1, \dots, \rho_N)$ . The physical feasibility constraints of the inertial parameters  $\boldsymbol{\theta}_i$  of the  $i$ -th link, summarized in Eq. (3.28), are satisfied if the pseudo inertia matrix

$$\mathbf{P}_i(\boldsymbol{\theta}_i) = f(\boldsymbol{\theta}_i) = \begin{bmatrix} \frac{1}{2}\text{tr}(\mathbf{I}_i)\mathbf{1} - \mathbf{I}_i & \mathbf{h} \\ \mathbf{h}^T & m \end{bmatrix} \in \mathcal{S}^4, \quad (3.29)$$

defined for each rigid body is symmetric positive-definite [104]. Note that  $\mathbb{1}$  is used to denote the  $3 \times 3$  identity matrix. The requirement that  $P_i(\theta_i) > 0$  implies the fully physically feasible inertial parameters are in the manifold  $S_{++}^4 = \{P_i(\theta_i) \in S^4 : P_i(\theta_i) > 0\}$ . For every rigid body  $i$  in the kinematic chain, there exist a pseudo inertia matrix [110]. Consequently, this means that the inertial parameters of a robot define a point  $\{P_i\}_{i=1}^N$  in the Riemannian product manifold  $\mathcal{M}^N$ .

### 3.4.4 Describing body shape: Robot mechanical topology

As outlined by Featherstone [87], the connectivity of a kinematic chain delineates the interconnection of its components, constituting what is known as the mechanical topology—essentially, the arrangement of joints and links. Understanding this topology is crucial as it serves as a foundational element for describing the body structure. Without this information, the individual geometry of the components lacks significance. Similarly, knowledge of only the inertial properties of each body in a kinematic chain is insufficient for describing the dynamics associated with their coupling. Therefore, a robotic agent must possess the capability to deduce the topology of its body before instantiating its kinematic and dynamic properties.

Having the topology of the body such relevance, the fact is that a scarce number of works have pondered the problem of how to learn it (see, for example, [54]). It seems reasonable to assume that this stems from the typical premise that this information is known a priori. Yet, a fully independent robotic agent that is to develop an understanding of its body through the development of a body schema needs to obtain this information exclusively by itself. This gains prominence as gradually robots become more adaptable and modular. Therefore, if there is access to the number and modalities of the robot's sensorimotor signals, an indication of the body topology must be extracted from them.

#### 3.4.4.1 Embodiment and information structure

To address the question of how the body's topology can be learned, this dissertation relies on the widely accepted hypothesis that the interaction of an embodied agent with its environment gives rise to statistical regularities in its sensorimotor signals [7, 65, 111, 112] (see Fig. 3.7). These statistical regularities, intertwined with the concept of sensorimotor contingencies [5], have been quantified using information-theoretic measures, which assess the information sharing among different modalities in the robot's sensorimotor system [113–117].

Fig. 3.8 illustrates how information structure in sensorimotor signals can emerge from embodiment. It depicts various bodies equipped with sensors (Fig. 3.8a), with these sensors acting as information sources having relationships that involve sharing information. The

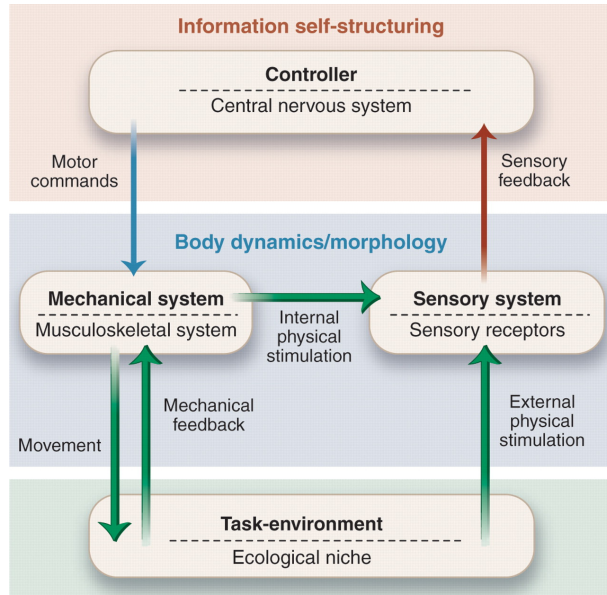


Figure 3.7: Implications of embodiment. From Pfeifer et al. [65]. Reprinted with permission from AAAS.

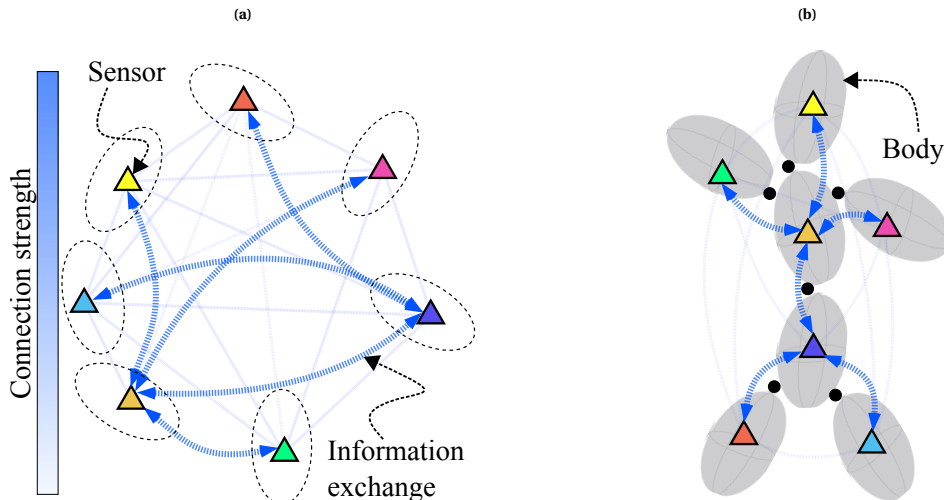


Figure 3.8: Embodiment and information structure. (a) Sensors on a robot exchange information at different strength levels. (b) This strength is associated with the embodiment of the robot, a kinematic tree in this case.

strength of these relationships is visually denoted by the blue lines (edges) connecting the sensors. Owing to the robot's morphology, stronger connections exist between specific sensors, as indicated by dark blue edges. These robust connections signify the body topology of the robot, illustrated in Fig. 3.8b, portraying a tree-like structure where the most substantial information sharing occurs between sensors in adjacent bodies. The key takeaway from this example is that the structure of the robot's body serves as a hypothesis for the strength of information sharing.

### 3.4.4.2 Fundamentals of graph theory

The sensorimotor relationships shown in Fig. 3.8 are an example of mathematical object known as a graph [118]. The mechanical topology of a robot can also be represented as a graph, whose connectivity represents the topology [87]. Therefore, it is important to introduce some fundamental concepts related to graph theory before proceeding with the discussion.

**Definition of a graph** A graph  $\mathcal{G} = (\mathcal{V}, \mathcal{E})$  is a mathematical construct that represents the interconnections between the elements of a system [118]. These elements are represented as a set  $\mathcal{V} = \{v_i\}_{i=1}^n$  of  $n$  nodes (also called *vertices*) and their connections are depicted as a set of edges  $\mathcal{E} = \{e_i\}_{i=1}^m \subseteq \mathcal{V} \times \mathcal{V}$ . Note that it is possible that an edge connects a node to itself, in which case the edge defines a self loop.

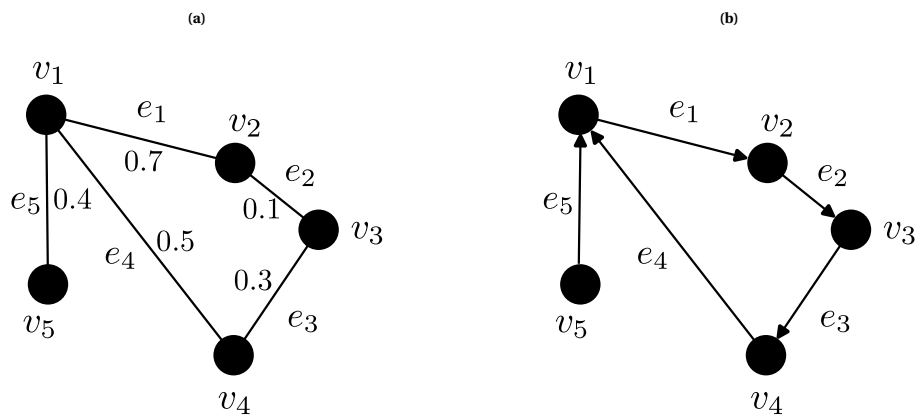


Figure 3.9: Two basic types of graphs. (a) An undirected and (b) a directed graph.

Two nodes  $i$  and  $j$  are said to be *adjacent* if there is an edge  $e$  connecting them. Similarly, the edge  $e$  connecting the nodes is called *incident* to  $i$  and  $j$ . For example, the nodes  $v_1$  and  $v_4$  in Fig. 3.9a are adjacent to each other and the edge  $e_4$  is incident to both nodes. The number of edges that are incident to a node is the *degree* of the vertex.

A *path* represents a potential sequence of edges connecting any two given nodes. The number of edges determines the *length* of the path. A graph is said to be *connected* if there is at least one path between every pair of nodes; otherwise, it is labeled *disconnected*. A *cycle* constitutes a path comprising a minimum of three edges, where the initial and final vertices are identical, and no vertices are repeated in between. Lastly, a graph is *complete* if there exists a path connecting every pair of nodes. Notice that the maximum number of edges in an undirected graph with  $n$  nodes is  $n(n - 1)/2$ .

An *undirected* graph lacks any specified direction assigned to its edges, meaning the connections between nodes are bidirectional. On the other hand, a *directed* graph, commonly

referred to as a *digraph*, introduces directionality to its edges. In a directed graph, each edge has an explicit direction, indicating a one-way flow from one node to another. This directional information adds an extra layer of complexity to the relationships within the graph, as opposed to the bidirectional nature of edges in an undirected graph.

A *weighted* graph  $\mathcal{G}(\mathcal{V}, \mathcal{E}, \mathbf{W})$  associates numerical value, a weight, to each edge. The weights with weights  $\mathbf{W} : \mathcal{V} \times \mathcal{V} \rightarrow \mathbb{R}_+$  express some quantitative measure such as distance, cost, time, or any other relevant metric depending on the context of the graph. Unlike an unweighted graph, where edges simply represent connections between nodes, a weighted graph provides additional information about the relationships between nodes. For a weighted graph, the *strength* of a vertex corresponds to the sum of the edge weights associated with it.

**Algebraic representation of a graph** A graph with  $n$  vertices can be represented as a square  $n \times n$  matrix  $\mathbf{A}$ . This algebraic representation is called the *adjacency matrix* and depicts the graph's connectivity pattern; that is, the elements of the matrix indicate whether pairs of vertices  $(i, j)$  are adjacent or not in the graph. Formally, the elements of a *binary* adjacency matrix  $\mathbf{A}$  are determined as follows

$$(\mathbf{A})_{i,j} = \begin{cases} 1 & \text{if and edge connects nodes } i \text{ and } j \\ 0 & \text{otherwise.} \end{cases} \quad (3.30)$$

By extension, a *weighted* adjacency matrix  $\mathbf{W}$  denotes a weighted connection for some of the  $(i, j)$  entries, i.e  $(\mathbf{W})_{i,j} \in \mathbb{R}_+$ . If the graph is undirected, the adjacency matrix is symmetric, which implies that  $\mathbf{A} = \mathbf{A}^\top$  and  $\mathbf{W} = \mathbf{W}^\top$  respectively. Note, however, that for the case of digraphs, the adjacency matrix is not necessarily symmetric. To illustrate this, refer to the graph in Fig. 3.9a, the corresponding binary and weighted adjacency matrices are

$$\mathbf{A} = \begin{bmatrix} 0 & 1 & 0 & 1 & 1 \\ 1 & 0 & 1 & 0 & 0 \\ 0 & 1 & 0 & 1 & 0 \\ 1 & 0 & 1 & 0 & 0 \\ 1 & 0 & 0 & 0 & 0 \end{bmatrix}$$

and

$$\mathbf{W} = \begin{bmatrix} 0 & 0.7 & 0 & 0.5 & 0.4 \\ 0.7 & 0 & 0.1 & 0 & 0 \\ 0 & 0.1 & 0 & 0.3 & 0 \\ 0.5 & 0 & 0.3 & 0 & 0 \\ 0.4 & 0 & 0 & 0 & 0 \end{bmatrix}.$$

Similarly, for the digraph in Fig. 3.9b, the adjacency matrix is

$$\mathbf{A}_D = \begin{bmatrix} 0 & 1 & 0 & 0 & 0 \\ 0 & 0 & 1 & 0 & 0 \\ 0 & 0 & 0 & 1 & 0 \\ 1 & 0 & 0 & 0 & 0 \\ 1 & 0 & 0 & 0 & 0 \end{bmatrix}.$$

Notice that unless there are self loops in the graph, the main diagonal of an adjacency matrix contains only zero entries. Two other important matrices related to a graph  $\mathcal{G}$  are the degree matrix  $\mathbf{D} : (\mathbf{D}_{ii}) = \sum_{j=1}^m w_{ij}$ , a diagonal matrix whose entries are the sum of the rows of  $\mathbf{W}$ , and the combinatorial graph Laplacian (CGL), defined as  $\mathbf{L}_{\text{CGL}} = \mathbf{D} - \mathbf{W}$  [119].

**The normalized adjacency matrix** The normalized adjacency matrix, defined as

$$\mathbf{W} = \mathbf{D}^{-\frac{1}{2}} \mathbf{W} \mathbf{D}^{-\frac{1}{2}}, \quad (3.31)$$

is particularly employed in spectral graph theory [120] and related analyses. Normalization helps account for variations in node degrees and provides a more balanced representation of the graph structure. One common application is in spectral clustering algorithms [?], where the normalized adjacency matrix is used to compute eigenvectors and eigenvalues, aiding in the identification of clusters or communities within a graph.

**Subgraphs and spanning trees** A *subgraph*  $\mathcal{G}_1$  is obtained by selecting a subset of the nodes of another graph  $\mathcal{G}$  and a corresponding subset of the edges connecting those nodes. Formally, a graph  $\mathcal{G}_1(\mathcal{V}_1, \mathcal{E}_1)$  is a subgraph of  $\mathcal{G}$  if and only if  $\mathcal{V}_1 \subseteq \mathcal{V}$  and  $\mathcal{E}_1 \subseteq \mathcal{E}$ . This is written  $\mathcal{G}_1 \subseteq \mathcal{G}$ . One particular subgraph of interest in this work are spanning trees. First, a *tree graph* is a graph that does not contain cycles. Such structure usually depicts a hierarchical arrangement. Consequently, a *spanning tree*  $\mathcal{G}_1$  of a graph  $\mathcal{G}$  is a subgraph containing all the nodes in  $\mathcal{G}$  and whose edges form a tree that defines paths that ensure that all the nodes remain connected. The edges of  $\mathcal{G}_1$  are denoted as the branches of the tree. In general, a graph  $\mathcal{G}_1$  is said to be a spanning subgraph of  $\mathcal{G}$  if and only if  $\mathcal{V}_1 = \mathcal{V}$  and  $\mathcal{E}_1 \subseteq \mathcal{E}$ . It is worth noting that every connected graph has a spanning tree and that there are  $n^{n-2}$  distinct spanning trees with  $n - 1$  edges on a connected graph with  $n$  vertices [118]. Examples of spanning trees are shown in Fig. 3.10.

**Minimum spanning tree and Kruskal's algorithm** The minimum spanning tree of an undirected, connected, and weighted graph is the spanning tree whose edge weight sum is less than or equal to that of all other spanning trees [121]. Kruskal's algorithm [122] is the stan-

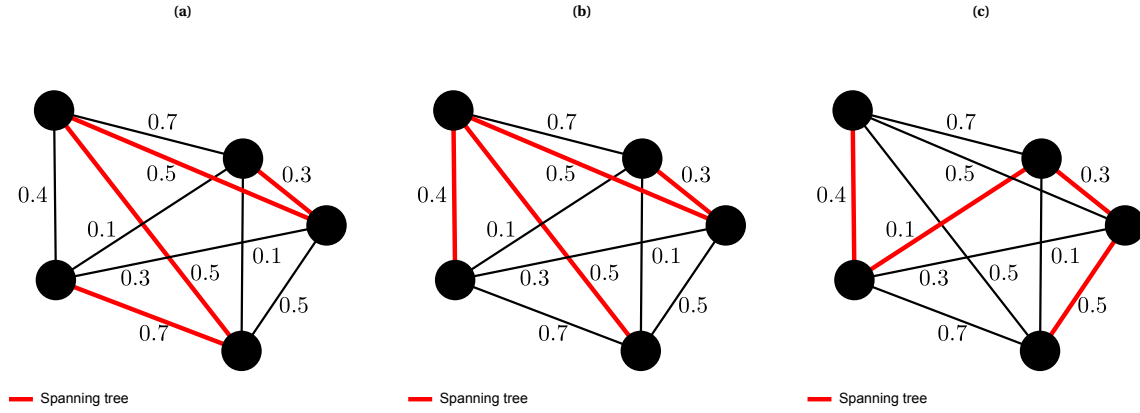


Figure 3.10: Different spanning trees for the same graph.

dard method to find the minimum spanning tree of a graph. In this work we use an equivalent concept, the *maximum spanning tree* (MST), which corresponds to the spanning tree with maximum edge weight sum.

**Metrics for graph comparison** Several works cover a number of metrics and measures to assess the similarity of any two given graphs. Commonly used metrics include eigenvalue distribution analysis [123, 124], and the graph adjacency spectral and matrix distances [125]. This dissertation will use the latter two measures as they allow the local and global comparison of the graph structure.

On the one hand, the spectral distance between two graphs  $\mathbf{W}_1$  and  $\mathbf{W}_2$  is simply the  $L_2$  norm of the difference between their spectra

$$d_s(\mathcal{G}_1, \mathcal{G}_2) = \sqrt{(\mathbf{s}^{\mathbf{W}_1} - \mathbf{s}^{\mathbf{W}_2})^\top (\mathbf{s}^{\mathbf{W}_1} - \mathbf{s}^{\mathbf{W}_2})}, \quad (3.32)$$

with spectrum of a graph  $\mathcal{G}$  defined as the vector  $\mathbf{s}^{\mathbf{W}}$  containing the eigenvalues  $s_k$  of its weighted adjacency matrix  $\mathbf{W}$  sorted in descending order; that is

$$\mathbf{s}^{\mathbf{W}} = [s_1, s_2, \dots, s_k, \dots, s_n]^\top. \quad (3.33)$$

On the other hand, the matrix distance expresses the a direct comparison of the pairwise affinities between the graphs  $\mathbf{W}_1$  and  $\mathbf{W}_2$ . From the many potential matrix distances, here the Frobenius distance is used; i.e,

$$d_{\mathbf{W}}(\mathcal{G}_1, \mathcal{G}_2) = \|\mathbf{W}_1 - \mathbf{W}_2\|_F. \quad (3.34)$$

### 3.4.4.3 Network topology inference

As mentioned before, the mechanical topology of a robot can be represented as a graph. The nodes in said graph correspond to the links and the edges indicate the joints connecting those bodies. how to obtain this graph remains unanswered. The relation between the robot morphology and information structure provides a starting point to search for the robot topology in the relationships among the sensorimotor signals. In general, the process of identifying and visually representing relationships among various elements within a system, based on the available measurements, is termed *network topology inference* (NTI) [126]. Unveiling the structure of a network or graph through topology learning facilitates the analysis of interactions among entities.

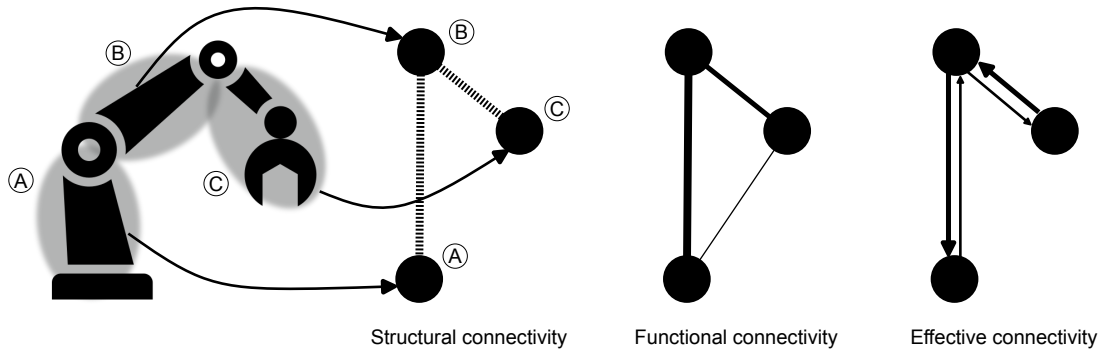


Figure 3.11: Types of connectivity. Every rigid body in the robot represents a node in the graphs.

**Types of connectivity** Often used in the field of neuroscience [127], three different types of connectivity are distinguished [128, 129]:

- **Structural Connectivity (SC).** Refers to the physical connections between different elements in a network. In the context of neuroscience, it typically involves the anatomical connections between brain regions. It is measured with techniques such as diffusion-weighted imaging (DWI) or diffusion tensor imaging (DTI) are commonly used to infer structural connectivity in the brain.
- **Functional Connectivity (FC).** Refers to the statistical dependencies or temporal correlations between the activity of different elements in a network. As explained in [130], FC is an information-theoretic metric that characterizes dependencies using probability distributions of observed signals. It can be categorized into non-directed and directed forms, with the latter being associated with statistical causation derived from the data [131].
- **Effective Connectivity (EC).** Specifically addresses the dynamic, state-dependent influence that one network element has on another within a particular causal dynamics

model. Essentially, effective connectivity denotes coupling or directed causal influence [128]. Exemplary applications of these concepts can be observed in the fields of biology [132] and neuroscience [127, 133].

A representation of the intricate relationships among the three types of connectivity is given in Fig. 3.11. It depicts a simple robot arm as an example. The nodes represent the three links that compose the robot. Regarding SC and FC, a nuanced connection exists, albeit not strictly one-to-one. For example, the SC reflect the actual physical composition of the body, three bodies connected by two joints (the edges in the SC graph). Sensory signals coming from these bodies might lead to potential functional interactions of varied degree (the edges in the FC graph) that have a foundation on the bodily structure of the robot; yet, it does not ensure their occurrence. Actually, functional relationships can appear even in the absence of direct structural connections, not the light edge between nodes  $A$  and  $C$  in the FC graph. Moving to EC and FC, the former extends the latter by seeking to model the direction and strength of influence between different elements. While FC identifies statistical associations, EC strives to unveil the underlying causal relationships, the directed edges in the EC graph. In summary, these three connectivity types are interrelated components in the complex landscape of NTI. Structural connections provide the anatomical substrate, functional connections depict statistical dependencies, and effective connections aspire to model causal relationships within the network.

**Inferring the connectivity** In NTI the elements  $\mathcal{V}$  of a graph  $\mathcal{G}$  are known but its connectivity (i.e. how these elements relate to each other) is unknown. The problem of learning the edges  $\mathcal{E}$  that best explain the relationships among the  $N_{\mathcal{V}}$  elements in  $\mathcal{V}$  leads to define a graph a graph  $\mathcal{G}(\mathcal{V}, \mathcal{E}, \mathbf{W})$  with an strictly positive weighted adjacency matrix  $\mathbf{W}$ . To find this matrix, a number of sample points  $m$  from the signals at the nodes  $\mathbf{x} = [x_1, x_2, \dots, x_{N_{\mathcal{V}}}]^{\top} \in \mathbb{R}^{N_{\mathcal{V}}}$  are collected into a data matrix  $\mathbf{X} \in \mathbb{R}^{N_{\mathcal{V}} \times m}$ . Using  $\mathbf{X}$  together with some prior knowledge, such as data distribution, the location of the sensors, the physical relationships between the signals, or the data similarity candidate graphs  $\mathcal{G}$  can be defined [126, 134]. Commonly, NTI methods are subdivided in statistical models, physically motivated models, and more recently, in methods from graph signal processing (GSP), see Fig. 3.12.

NTI methods based on statistical models aim to capture signal similarities, utilizing measures such as the Pearson correlation, Jaccard coefficient, Gaussian radial basis functions, and mutual information. The predominant approach involves expressing these similarities by computing the correlation of the data matrix  $\mathbf{X}$  and assuming joint Gaussianity of the variables. The primary objective is usually to estimate the graph structure embedded in the precision matrix (defined as the inverse of the covariance matrix). However, as the precision matrix is not a proper adjacency matrix, methods have been developed to ensure Laplacian constraints (to find a valid graph) and structural constraints (to promote sparsity). Notable

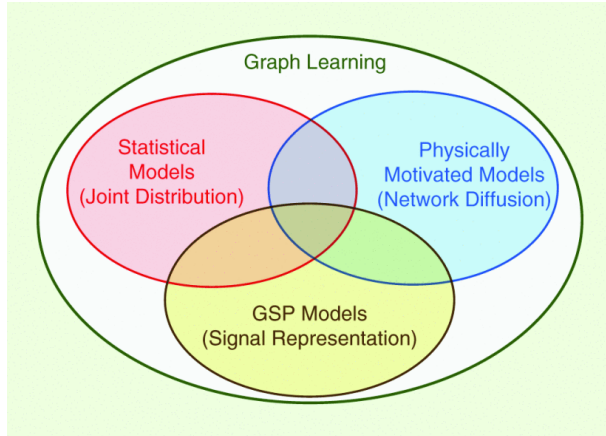


**Figure 3.12: Different methods for NTI.** Image taken from [126].

examples include the graphical LASSO [135] and the work in [117, 136]. Information theory is pivotal in NTI, providing a robust framework for deducing network structures through fundamental concepts like mutual information. Numerous methodologies rooted in information theory have been proposed for network inference [114, 137–139]. In NTI motivated by psychical models the structure of  $\mathcal{G}$  is assumed to be tied to an underlying physical phenomenon or process on the graph; for example, network diffusion processes or information propagation models. Finally, in GSP-based NTI, the vector of node signals  $x$  at any given time is deemed a graph signal and is hypothesized to be a function of some process that depends on the graph; i.e.,  $\mathbf{X} = f(\mathcal{G})$ . In GSP, each of the vectors  $x$  is considered a signal defined on the nodes of the weighted graph  $\mathcal{G}$ . Learning this graph implies determining an adjacency  $\mathbf{W}$  such that  $f(\mathcal{G})$  reflects some features in the data matrix  $\mathbf{X}$ . Examples involve learning graphs from observations of smooth signals and identifying the structure of network diffusion processes.

Of particular interest to this dissertation are the statistical methods based on information theoretic measures to determine the functional connectivity among the robot sensorimotor signals. The belief is that the FC found through these methods should be in agreement with the embodiment and information structure hypothesis and, thus, should lead to the discovery of the robot mechanical topology (which is analogous to the structural connectivity).

#### 3.4.4.4 Basics of information theory

Recapitulating, the construction of a body schema necessitates an understanding of the body's topology. As discussed in Section 3.4.4.3, a graph that represents the organization of the robot's joints and links functions as a depiction of its structural connectivity. However, given the available information, restricted to the number and modalities of the sensorimotor signals, the deduction of this structural connectivity must occur from the potential relationships among these signals.

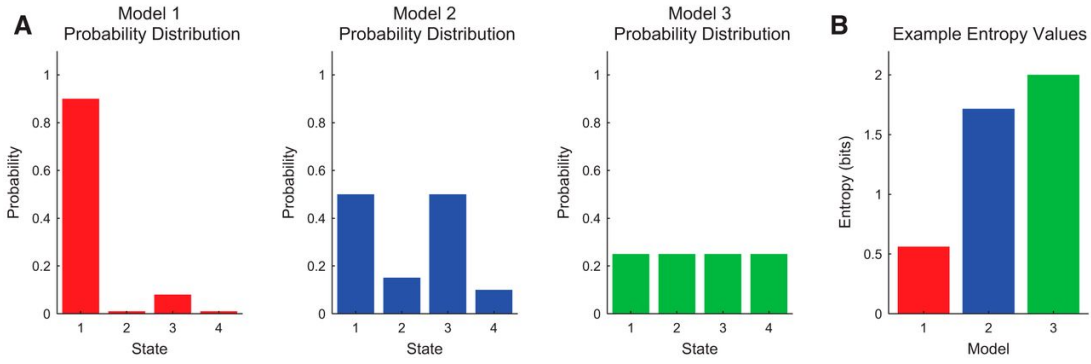


**Figure 3.13: Entropy of three example distributions.** The closer the distributions resemble a uniform distribution, the more information they contain. Image taken from [141].

In Section 3.4.4.1, the emphasis was on the fact that the robot’s morphology shapes the information structure of sensorimotor signals. Consequently, representing this structure as a graph corresponds to the inference of the functional connectivity among the robot signals. Specifically, FC among sensorimotor signals can be captured using measures from information theory [140]. These measures are general, as they are not tied to a specific model, and expressive, enabling the capture of statistical relationships of both linear and nonlinear nature.

**Entropy of random variables** The entropy of a random variable is a function which attempts to characterize the average uncertainty or unpredictability of a random variable. It is often used to quantify the amount of information in a random process. Formally, the entropy of a variable  $X$  is a function of its probability distribution and is defined as

$$H(X) = - \sum_{i=1}^n p(x_i) \log_2(p(x_i)). \quad (3.35)$$

Similarly, the joint entropy between two random variables  $X$  and  $Y$  is dependent on the joint probability of the two variables; i.e,

$$H(X, Y) = - \sum_{i=1}^n \sum_{j=1}^n p(x_i, y_j) \log_2(p(x_i, y_j)). \quad (3.36)$$

In loose terms, entropy can be associated with the amount of information that a random variable conveys. This is exemplified in Fig. 3.13, where three probability distributions are displayed. Essentially, the less uniform the corresponding probability distribution, the less entropy it has, and hence the more information it provides; i.e. larger entropy value.

**Mutual Information** The mutual information (MI) measures the amount of information that one random variable provides about another random variable. Conversely, it quantifies the reduction in uncertainty about one variable due to knowledge of the other. The MI

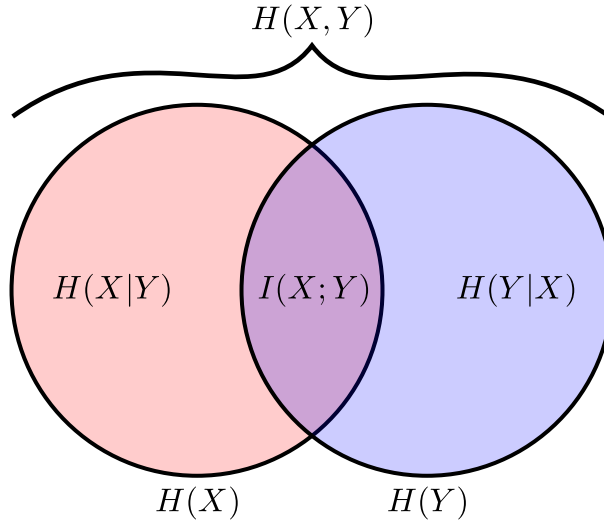


**Figure 3.14: Relation between entropy and mutual information.** The mutual information between two variables expresses the amount of information that one variable contains about the other.

between two random variables is a symmetric measure of information computed as the relative entropy (also known as Kullback-Leibler divergence) of the joint probability distribution  $p(x,y)$  and the product of the marginal probability distributions  $p(x)$  and  $p(y)$ ; that is,

$$I(X;Y) = \sum_{x \in \mathcal{X}} \sum_{y \in \mathcal{Y}} p(x,y) \log_2 \frac{p(x,y)}{p(x)p(y)}. \quad (3.37)$$

Basically, this expression is comparing how similar is the joint distribution to the product of the marginals. If they are the same,  $X$  and  $Y$  are independent and there is no information that one can tell about the other; in other words, the MI between them is zero. Alternatively, the MI can be expressed in terms of the entropy and joint entropy as follows

$$I(X;Y) = I(Y;X) = H(X) + H(Y) - H(X,Y), \quad (3.38)$$

where it is clear why the MI is symmetric; it represents the information shared by the two random variables, see Fig. 3.14.

**Connection to correlation** It is worth dedicating some time to discuss using mutual information against the well-known correlation. Both have the common objective of evaluating the interdependence between random variables. Correlation measures the intensity and directionality of a linear association between two variables, whereas MI can identify any statistical dependency—including non-linear associations. Therefore, MI represents a more comprehensive measure of the connection between variables compared to correlation, rendering it a valuable instrument to express the relations between sensorimotor variables.

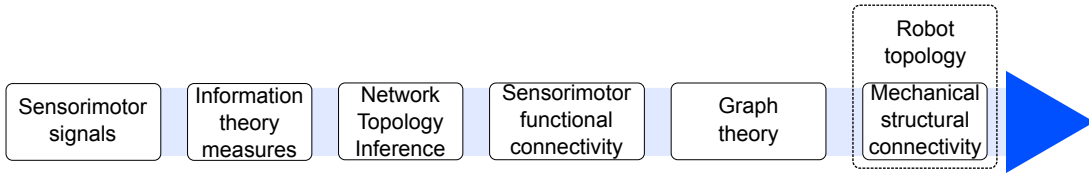


**Figure 3.15: Topology inference process.** Extracting the robot's mechanical topology from the relationships among the sensorimotor signals involves combining tools from information and graph theory to determine the functional connectivity between signals and using it to infer the mechanical structural connectivity.

#### 3.4.4.5 Summary

The mechanical arrangement of the robot's joints and links referred to as topology, constitutes a crucial element of the robot body schema, playing a fundamental role in fully characterizing its kinematic and dynamic properties. As illustrated in Fig. 3.15, a robotic agent's autonomous acquisition of body topology necessitates reliance on the information structure embedded in its sensorimotor signals. The unveiling of this structure entails thoroughly examining the relationships among the sensorimotor signals using information theory measures. Once these measures are established, they can be utilized to infer the functional connectivity among the signals. In the subsequent chapter, we delve into the final step, wherein graph theory tools and first-order kinematic principles are employed to ascertain the mechanical structural connectivity based on sensorimotor functional connectivity.

### 3.4.5 Learning and adaption of the body properties

#### 3.4.5.1 Learning completes the robot body schema

Model-based robotics is inherently linked to the concept of the body schema, as defined in Def. 3.1. The methods presented so far in this chapter encompass a theoretical foundation to model the physical properties of robots. However, these methods often treat body properties as immutable, relying on a single identification or calibration procedure, and often dependent on external (off-body) measurement devices. Some studies have compared the conventional characteristics of model-based robotics, such as being amodal, fixed, explicit, centralized, and modular, with the properties of a biological body schema [76]. Unlike robotic body models, the body schema is dynamic, capable of modification based on experiences, learning, and changes in the body itself. Additionally, biological systems are inherently self-learning and rely on the integration of multi-modal sensory information [67].

Leveraging proprioceptive embodied sensors and integrating machine learning techniques with model-based robotics allows turning the problems of instantiating the topology, kinematics, and inertial description of a robot into incremental learning problems. Such a synergistic combination can provide traditional model-based body representations with the plasticity required to enable robots to construct, monitor, and adjust their understanding of their bodies by integrating information from multiple sensory modalities.

### 3.4.5.2 Offline and online learning

In the realm of machine learning, online learning and offline learning represent distinct approaches to model training. Online learning, or incremental learning, involves learning the model as new data becomes available, typically processing one observation at a time. In this scenario, the learning algorithm's parameters are updated after each individual training instance, making it particularly advantageous for systems dealing with a continuous flow of data that must rapidly adapt to changing conditions. On the other hand, offline learning, also known as batch learning, entails training the model over all observations in a dataset simultaneously. The model is trained with a static dataset, and the parameters are updated once the learning process is complete for the entire dataset.

Offline learning (i.e. offline optimization) is more aligned with the context of model-based robotics. To truly make the transition to a robot body schema online (incremental) learning needs to be the fundamental philosophy to learning the properties of the body schema. In this dissertation modern variations of gradient descent will be considered as the driving mechanism behind the learning and adaption of the attributes of the robot morphology.

### 3.4.5.3 Fundamentals of gradient descent

Gradient descent (GD) is in essence an optimization algorithm to sequentially minimize a *cost function*  $J(\mathbf{x})$  with respect to a given set of parameters  $\mathbf{x} \in \mathbb{R}^d$  moving in the direction opposite to its gradient  $\nabla_{\mathbf{x}} J(\mathbf{x})$  at the current point  $\mathbf{x}_k$ . GD is considered a local optimizer as it primarily finds a local minimum of  $J$ . The algorithm can be summarized in a iterative process expressed in the simple equation

$$\mathbf{x}_{k+1} = \mathbf{x}_k - \eta \nabla_{\mathbf{x}_k} J(\mathbf{x}_k; \mathcal{D}), \quad (3.39)$$

which gives the update  $\mathbf{x}_{k+1}$  to the optimization variables using a *learning rate*  $\eta$  that controls the size of the step given in the negative direction of the gradient. If this hyperparameter is too small, the updates  $\mathbf{x}_{k+1}$  will differ slightly from  $\mathbf{x}_k$  and convergence will take a long time. On the contrary, if  $\eta$  is too large, the parameter updates may oscillate around a local optima and even diverge. From the number of data points from an already-collected dataset  $\mathcal{D}$  that are used to represent the optimization cost function  $J$ , three variants of GD are typical: batch, stochastic, and mini-batch GD. If all data in  $\mathcal{D}$  is used to compute the gradient, it is called batch GD. It relies on a static dataset and substantial computational resources (CPU, memory, and storage) for training and thus lacks the flexibility to adapt incrementally to new data. This inability to incorporate new observations in real-time hinders its applicability for online learning in dynamic environments with constantly evolving data streams.

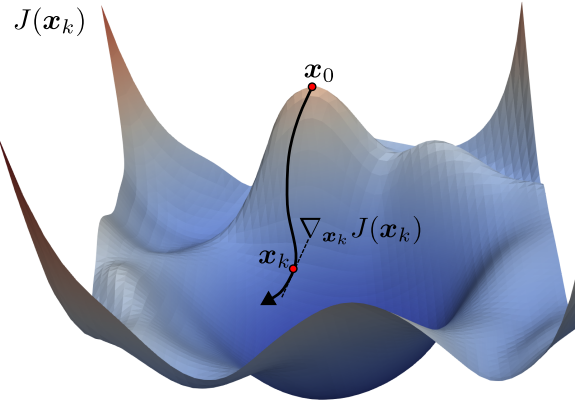


**Figure 3.16: Concept art gradient descent.** Image credits: <https://www.cs.umd.edu/~tomg/projects/landscapes/>

Stochastic Gradient Descent (SGD) [142] serves as a simplification of batch GD and is widely employed machine in machine learning for online learning due to its efficiency with large-scale datasets and its ability to adapt to new data one observation at a time. Its advantages lie in its speed, processing quicker parameter updates, and memory efficiency. A recent review [143] discusses the properties of SGD as a standard optimization algorithm in deep learning. Despite its ability to escape local minima, the noisy updates of SGD and bouncing behavior near the minimum can yield good but non-optimal solutions [REF](#). When the gradient of the cost function is computed using a small subset or mini-batch of  $\mathcal{D}$ , rather than a single example or the entire dataset, SGD becomes mini-batch GD. This approach reduces the noise in the parameter updates compared to SGD, leading to more stable convergence. It allows for computational efficiency as the mini-batch can be processed in parallel, and it is typically faster than batch GD for convergence.

#### 3.4.5.4 Improved gradient descent

The challenges associated with standard (commonly named vanilla) GD encompass critical issues. First, there is the already mentioned sensitivity to the selected learning rate  $\eta$ . Noisy gradients are a particular problem of SGD and mini-batch GD. These may lead to slower and less stable training compared to batch GD. The algorithms may also encounter obstacles like local minima and saddle points, particularly problematic in non-convex optimization problems, hindering the discovery of the global minimum.

Various improvements have been proposed to improve vanilla GD in recent years [143, 144]. Noteworthy among these enhancements are the incorporation of a momentum term, adaptive learning rate mechanisms, and measures to handle very small step sizes. The momentum term, functioning as a moving average over past gradients, serves to smooth out steps in gradient descent, thereby mitigating oscillations and expediting convergence. Its purpose is to combat issues such as bouncing around the search space and getting stuck in

flat regions, ultimately elevating the optimization algorithm's efficacy and yielding superior final results.

The adaptive learning rate, tailored individually for each parameter based on the square root of the sum of the squares of historical gradients, facilitates larger updates for infrequent parameters and smaller updates for frequent ones. This adaptability proves beneficial for handling sparse data and managing sparse gradients. The approach aims to expedite convergence in the presence of sparse data by adjusting the learning rate according to the loss function's geometry. This allows for swift convergence in steep gradient directions and more cautious updates in flatter gradient directions.

However, a notable drawback of learning rate adaption is the its potential reduction to infinitesimally small values over time, limiting the ability to acquire additional knowledge. To counteract this issue, a decaying average of squared gradients was proposed to adjust the step size for each parameter. This adaptive strategy stabilizes the learning process, preventing oscillations in the optimization trajectory and proving effective for non-convex optimization problems commonly encountered in machine learning.

The following, three modern variants of gradient descent used in this dissertation are briefly discussed.

**Adaptive moment estimation: Adam** Adaptive Moment Estimation GD, commonly known as Adam [145], has become a powerful optimization technique standard in machine learning. Adam is an adaptive learning algorithm that refines SGD approach by incorporating both first-order moment estimates ( $m_t$ ) and second-order moment estimates ( $v_t$ ) of the gradients; that is

$$\begin{aligned} m_k &= \beta_1 m_{k-1} + (1 - \beta_1) \nabla_{\mathbf{x}_k} J(\mathbf{x}_k; \mathcal{D}) \\ v_k &= \beta_2 v_{k-1} + (1 - \beta_2) (\nabla_{\mathbf{x}_k} J(\mathbf{x}_k; \mathcal{D}))^2, \end{aligned} \tag{3.40}$$

where the moving averages of the momentum term and the squared gradients is adjusted via the discount factors  $\beta_1 \in [0, 1]$  and  $\beta_2 \in [0, 1]$ . The adaptive nature of Adam stems from dynamically adjusting learning rates  $\{\eta_i\}_{i=1}^d$  for each parameter based on the historical gradient information. This feature addresses a longstanding challenge in machine learning—manual tuning of learning rate  $\eta$ . The ability of Adam to autonomously adjust rates during training alleviates the need for meticulous parameter tuning, a characteristic that sets it apart from its predecessors.

A fundamental strength of Adam lies in its incorporation of momentum, which enables Adam to persist in the correct direction, surmounting obstacles such as flat regions or saddle points in the cost function  $J$ . Furthermore, Adam introduces a bias correction mechanism, particularly beneficial in the initial stages of training when moment estimates might be im-

precise\*. This correction, computed as

$$\begin{aligned}\hat{m}_k &= \frac{m_k}{1 - \beta_1} \\ \hat{v}_k &= \frac{v_k}{1 - \beta_2},\end{aligned}\tag{3.41}$$

enhances the accuracy of the mean and uncentered variance estimates in (3.40), contributing to the algorithm's robustness. The update rule for Adam, based on Eqs. (3.41) and (3.40), yields

$$x_{k+1} = x_k - \frac{\eta}{\sqrt{\hat{v}_t + \epsilon}} \hat{m}_t.\tag{3.42}$$

Note that according to [145], the default values of  $\beta_1 = 0.9$ ,  $\beta_2 = 0.999$ , and  $\epsilon = 10^{-8}$  seem to work well in practice.

Adam's computational efficiency is a standout feature, showcasing its prowess in a diverse array of applications. It has demonstrated a tendency to converge faster and demand less hyperparameter tuning than traditional SGD. Notably, Adam's adaptability to sparse or high-dimensional data renders it well-suited for complex models where different parameters may necessitate varying learning rates. This adaptability is particularly advantageous in real-world scenarios where data is inherently noisy.

The algorithm's ability to handle noisy gradients effectively speaks to its stability during training, contributing to the robustness that makes Adam a preferred choice in modern machine learning applications.

**AMS gradient descent** AMSGrad is a gradient descent method that aims at convergence issues faced by Adam and its variations [146]; which have been observed to exhibit issues related to the learning rate, where it may become too aggressive and lead to poor convergence behavior in certain scenarios. AMSGrad tries to address this issue by modifying the way it updates the parameters.

The key improvement introduced by AMSGrad lies in its handling of the adaptive learning rates for each parameter. In the original Adam algorithm, the learning rates are adapted based on the exponential moving averages of the first-order moment (mean) and the second-order moment (uncentered variance) of the gradients. However, Adam does not incorporate a mechanism to correct the bias in the estimate of the second-order moment, which can lead to an overly aggressive decrease in the learning rates.

AMSGrad addresses this limitation by modifying the update rule for the moving average of the second-order moment. Unlike Adam, AMSGad maintains a running average of the past squared gradients for each parameter without bias correction. Particularly, instead of using  $\hat{v}_t$  as in (3.41), its previous value  $\hat{v}_{k-1}$  is used as long as it is greater than the current

---

\*The terms  $v_k$  and  $m_k$  are biased towards their zero initial value.

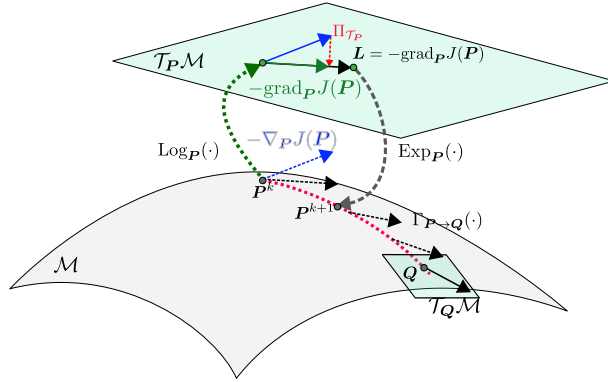


**Figure 3.17: Gradient descent on a manifold.** The figure illustrates the curved space of the manifold and its associated tangent space. The logarithmic and exponential maps enable to project a point from the tangent space to the manifold space and vice-versa.

value computed according to (3.40); i.e.,

$$\hat{v}_t = \max(\hat{v}_{t-1}, v_t). \quad (3.43)$$

The update rule for AMSGrad

$$x_{k+1} = x_k - \frac{\eta}{\sqrt{\hat{v}_t + \epsilon}} m_t \quad (3.44)$$

excludes also the regularization of the first momentum term. The alteration to the second moment ensures that the denominator in the learning rate calculation does not become excessively small over time, preventing the learning rate from growing uncontrollably small.

In essence, AMSGrad aims to provide a more stable and consistent learning rate, preventing scenarios where the learning rate diminishes rapidly and adversely affects convergence. By addressing this issue, AMSGrad aims to offer improved convergence behavior and generalization, particularly in cases where Adam might exhibit erratic behavior due to the uncorrected bias in the second-order moment estimate.

**Gradient descent on Riemannian manifolds** The gradient descent methods discussed above are thought to operate in Euclidean (flat) spaces. Some of the operators and quantities that describe the kinematics and dynamics of a robot are elements of curved manifold spaces and hence are more difficult to update following the update rules of Euclidean gradient descent methods. Considering again a cost function  $J(\mathbf{P})$ , the *Riemannian gradient* at a point  $\mathbf{P}$  in a manifold space  $\mathcal{M}$  is the orthogonal projection of the gradient in ambient Euclidean space

$$\mathbf{G} = \nabla J(\cdot) = \frac{\partial J}{\partial \mathbf{P}} \in \mathbb{R}^{n \times n} \quad (3.45)$$

onto the associated tangent space  $T_{\mathbf{P}} \mathcal{M}$  [147]; that is,

$$\text{grad}_{\mathbf{P}} J(\mathbf{P}) = \Pi_{T_{\mathbf{P}} \mathcal{M}} (\nabla J(\mathbf{P})) \in T_{\mathbf{P}} \mathcal{M}, \quad (3.46)$$

with the projection operator defined as

$$\Pi_{\mathcal{T}_P}(\mathbf{G}) \triangleq P \left( \frac{\mathbf{G} + \mathbf{G}^T}{2} \right) P, \quad (3.47)$$

for all the points in the manifold [148]. As described in [149], Riemannian gradient descent uses

$$\mathbf{P}^{k+1} = \text{Exp}_{\mathbf{P}^k} \left( -\gamma \text{grad}_{\mathbf{P}^k} J(\mathbf{P}^k) \right), \quad (3.48)$$

with  $\gamma \in (0, 1]$ , to compute the update to the parameter  $\mathbf{P}$  on  $\mathcal{M}$ . The exponential map  $\text{Exp}_{\mathbf{P}^k}(\cdot)$  of a Riemannian manifold at a point  $\mathbf{P}^k$  projects a point on the tangent space to the manifold space; i.e.,  $\text{Exp}_{\mathbf{P}^k} : \mathcal{T}_{\mathbf{P}^k} \mathcal{M} \rightarrow \mathcal{M}$ . Conversely, the logarithmic map takes a point on the manifold and projects it onto the associated tangent space; that is,  $\text{Log}_{\mathbf{P}^k} : \mathcal{M} \rightarrow \mathcal{T}_{\mathbf{P}^k} \mathcal{M}$ . Fig. 3.17 illustrates these maps and their involvement in Riemannian gradient descent. The particular definitions for the exponential and logarithmic maps depend on the considered Riemannian manifold  $\mathcal{M}$ .

Inspired by the stability and convergence speed of AMSGrad, this thesis utilizes its Riemannian counterpart, referred to as RAMSGrad for short [150]. Essential features of RAMSGrad encompass the computation of moving averages for the gradient and its Riemannian norm, as well as the amalgamation of previous gradients, taking into account the curvature of the manifold. A more detailed discussion of this algorithm will be provided in the upcoming chapter.

## 3.5 Chapter summary

This chapter offers an overview of various concepts related to the physical structure of the robot. It delves into the physical self and its connections to embodiment, body morphology, and body schema. Special focus is given to the body schema, serving as a model representation of the robot's physical structure. The chapter discusses its key features and establishes connections to model-based robotics, presenting the definition of the robot body schema utilized in this dissertation. Essential bodily features required for constructing the robot body schema are outlined, and methods for representing its kinematics and dynamics, encompassing the description of body size and inertial properties, are examined. Emphasis is placed on body shape, defined as the mechanical arrangement of joints and links, i.e., the body topology, crucial for characterizing kinematic and dynamic features. Concepts from information and graph theory are introduced to illustrate how performing network topology inference on the robot's sensorimotor signals can infer mechanical structural connectivity. Lastly, the chapter revisits modern implementations of gradient descent, particularly relevant in implementing online learning schemes to extract features of the robot body schema.

# 4

## Methods: How to learn the robotic body schema

We envision learning the robotic body schema as a series of learning stages that the robot must go through to discover core features of its body morphology. These features are part of the set

$$\mathcal{S} = \{N, \mathcal{G}, \mathbf{A}, \boldsymbol{\lambda}, \boldsymbol{\theta}\}, \quad (4.1)$$

whose elements are the number of bodies  $N$  in the kinematic chain, the graph  $\mathcal{G}$  that describes the sensorimotor interactions that result from the robot's embodiment, the adjacency matrix  $\mathbf{A}$  that captures the topology —mechanical arrangement of the bodies and joints—, its kinematic description (basic geometry)  $\boldsymbol{\lambda}$ , and the inertial parameters of the links  $\boldsymbol{\theta}$ . Thus, a robot capable of acquiring knowledge of the elements of  $\mathcal{S}$  is an agent that builds an understanding of its physical self. An overview of this process is depicted in Fig. S1.



# 5

## Results



# 6

## Discussion

The results and approach presented in this work bear resemblance to the work by Sturm [42], Hersch [37], Bongard [54], and Lipson [41]



# Bibliography

- [1] M. Kawato, “Internal models for motor control and trajectory planning,” *Current Opinion in Neurobiology*, vol. 9, no. 6, pp. 718–727, 1999. [Online]. Available: <https://www.sciencedirect.com/science/article/pii/S0959438899000288>
- [2] C. Pierella, M. Casadio, S. Solla, and F. A. Mussa-Ivaldi, “The dynamics of motor learning through the formation of internal models,” *PLoS Comput. Biol.*, 2019. [Online]. Available: <https://www.semanticscholar.org/paper/86924f6d980a37f579a9074209ea2fdb2c2ab5e8>
- [3] D. Nguyen-Tuong and J. Peters, “Model learning for robot control: a survey,” *Cognitive processing*, vol. 12, no. 4, pp. 319–340, 2011.
- [4] A. Maye and A. K. Engel, “Extending sensorimotor contingency theory: prediction, planning, and action generation,” *Adaptive Behavior*, vol. 21, no. 6, pp. 423–436, 2013.
- [5] L. Jacquy, G. Baldassarre, V. G. Santucci, and K. O'Regan, “Sensorimotor contingencies as a key drive of development: from babies to robots,” *Frontiers in Neurorobotics*, vol. 13, p. 98, 2019.
- [6] T. Buhrmann, E. A. Di Paolo, and X. Barandiaran, “A dynamical systems account of sensorimotor contingencies,” *Frontiers in psychology*, vol. 4, p. 285, 2013.
- [7] R. Pfeifer and J. Bongard, *How the body shapes the way we think: a new view of intelligence*. MIT press, 2006.
- [8] O. Holland and R. B. Goodman, “Robots with internal models a route to machine consciousness,” 2003. [Online]. Available: <https://api.semanticscholar.org/CorpusID:61034738>
- [9] S. Thrun, “Probabilistic robotics,” *Communications of the ACM*, vol. 45, no. 3, pp. 52–57, 2002.
- [10] I. Goodfellow, Y. Bengio, and A. Courville, *Deep Learning*. MIT Press, 2016, <http://www.deeplearningbook.org>.

- [11] B. Baker, O. Gupta, N. Naik, and R. Raskar, “Designing neural network architectures using reinforcement learning,” in *5th International Conference on Learning Representations*, 2017.
- [12] T. Elsken, J. H. Metzen, and F. Hutter, “Neural architecture search: A survey,” *The Journal of Machine Learning Research*, vol. 20, no. 1, pp. 1997–2017, 2019.
- [13] M. Matteucci, “Elearnt: Evolutionary learning of rich neural network topologies,” Carnegie Mellon University, Tech. Rep., 2006.
- [14] M. Rocha, P. Cortez, and J. Neves, “Simultaneous evolution of neural network topologies and weights for classification and regression,” in *International Work-Conference on Artificial Neural Networks*. Springer, 2005, pp. 59–66.
- [15] S. He, “Topological optimisation of artificial neural networks for financial asset forecasting,” Ph.D. dissertation, The London School of Economics and Political Science (LSE), 2015.
- [16] T.-Y. Kwok and D. Y. Yeung, “Constructive feedforward neural networks for regression problems: A survey,” Tech. Rep., 1995.
- [17] S. Lawrence, C. L. Giles, and A. C. Tsoi, “What size neural network gives optimal generalization? convergence properties of backpropagation,” Tech. Rep., 1998.
- [18] H. A. Talebi, F. Abdollahi, R. V. Patel, and K. Khorasani, “Neural network-based system identification schemes,” in *Neural Network-Based State Estimation of Nonlinear Systems*. Springer, 2010, pp. 37–59.
- [19] S. Urolagin, P. KV, and N. Reddy, “Generalization capability of artificial neural network incorporated with pruning method,” *Advanced computing, networking and security*, pp. 171–178, 2012.
- [20] S. S. Tirumala, S. Ali, and C. P. Ramesh, “Evolving deep neural networks: A new prospect,” in *Natural Computation, Fuzzy Systems and Knowledge Discovery (ICNC-FSKD), 2016 12th International Conference on*. IEEE, 2016, pp. 69–74.
- [21] S. Srinivas and V. Babu, “Learning neural network architectures using backpropagation,” in *Proceedings of the British Machine Vision Conference (BMVC)*, E. R. H. Richard C. Wilson and W. A. P. Smith, Eds. BMVA Press, September 2016, pp. 104.1–104.11. [Online]. Available: <https://dx.doi.org/10.5244/C.30.104>
- [22] E. Castillo, N. Sánchez-Marcano, A. Alonso-Betanzos, and C. Castillo, “Functional network topology learning and sensitivity analysis based on anova decomposition,” *Neural computation*, vol. 19, no. 1, pp. 231–257, 2007.

- [23] D. Nguyen-Tuong, J. Peters, M. Seeger, and B. Schölkopf, “Learning inverse dynamics: a comparison,” in *European Symposium on Artificial Neural Networks*, no. EPFL-CONF-175477, 2008.
- [24] D. Nguyen-Tuong and J. Peters, “Using model knowledge for learning inverse dynamics,” in *Robotics and Automation (ICRA), 2010 IEEE International Conference on*. IEEE, 2010, pp. 2677–2682.
- [25] M. Atencia and G. Joya, “Hopfield networks: from optimization to adaptive control,” in *Neural Networks (IJCNN), 2015 International Joint Conference on*. IEEE, 2015, pp. 1–8.
- [26] Q. Zhu and S. Mao, “Inertia parameter identification of robot arm based on bp neural network,” in *Control Conference (CCC), 2014 33rd Chinese*. IEEE, 2014, pp. 6605–6609.
- [27] V. Bargsten, J. de Gea Fernandez, and Y. Kassahun, “Experimental robot inverse dynamics identification using classical and machine learning techniques,” in *ISR 2016: 47st International Symposium on Robotics; Proceedings of*. VDE, 2016, pp. 1–6.
- [28] P. Christiano, Z. Shah, I. Mordatch, J. Schneider, T. Blackwell, J. Tobin, P. Abbeel, and W. Zaremba, “Transfer from simulation to real world through learning deep inverse dynamics model,” *arXiv preprint arXiv:1610.03518*, 2016.
- [29] L. Yan and C. J. Li, “Robot learning control based on recurrent neural network inverse model,” *Journal of Field Robotics*, vol. 14, no. 3, pp. 199–212, 1997.
- [30] A. S. Polydoros, L. Nalpantidis, and V. Krüger, “Real-time deep learning of robotic manipulator inverse dynamics,” in *Intelligent Robots and Systems (IROS), 2015 IEEE/RSJ International Conference on*. IEEE, 2015, pp. 3442–3448.
- [31] H. A. Pierson and M. S. Gashler, “Deep learning in robotics: a review of recent research,” *Adv. Robotics*, vol. 31, no. 16, pp. 821–835, 2017.
- [32] N. Sünderhauf, O. Brock, W. J. Scheirer, R. Hadsell, D. Fox, J. Leitner, B. Upcroft, P. Abbeel, W. Burgard, M. Milford, and P. Corke, “The limits and potentials of deep learning for robotics,” *Int. J. Robotics Res.*, vol. 37, no. 4-5, pp. 405–420, 2018.
- [33] A. R. Geist and S. Trimpe, “Structured learning of rigid-body dynamics: A survey and unified view from a robotics perspective,” *GAMM-Mitteilungen*, vol. 44, no. 2, p. e202100009, 2021. [Online]. Available: <https://onlinelibrary.wiley.com/doi/abs/10.1002/gamm.202100009>

- [34] M. Lutter and J. Peters, “Combining physics and deep learning to learn continuous-time dynamics models,” *The International Journal of Robotics Research*, vol. 42, no. 3, pp. 83–107, 2023.
- [35] P. D. Nguyen, Y. K. Georgie, E. Kayhan, M. Eppe, V. V. Hafner, and S. Wermter, “Sensorimotor representation learning for an “active self” in robots: a model survey,” *KI-Künstliche Intelligenz*, pp. 1–27, 2021.
- [36] M. Hoffmann, H. Marques, A. Arieta, H. Sumioka, M. Lungarella, and R. Pfeifer, “Body schema in robotics: a review,” *IEEE Transactions on Autonomous Mental Development*, vol. 2, no. 4, pp. 304–324, 2010.
- [37] M. Hersch, E. Sauser, and A. Billard, “Online learning of the body schema,” *International Journal of Humanoid Robotics*, vol. 5, no. 02, pp. 161–181, 2008.
- [38] R. Martinez-Cantin, M. Lopes, and L. Montesano, “Body schema acquisition through active learning,” in *2010 IEEE international conference on robotics and automation*. IEEE, 2010, pp. 1860–1866.
- [39] J. W. Hart and B. Scassellati, “A robotic model of the ecological self,” in *Humanoid Robots (Humanoids), 2011 11th IEEE-RAS International Conference on*. IEEE, 2011, pp. 682–688.
- [40] H. Lipson, “Task-agnostic self-modeling machines,” *Sci. Robotics*, vol. 4, no. 26, 2019.
- [41] B. Chen, R. Kwiatkowski, C. Vondrick, and H. Lipson, “Fully body visual self-modeling of robot morphologies,” *Sci. Robotics*, vol. 7, no. 68, 2022.
- [42] J. Sturm, C. Plagemann, and W. Burgard, “Body schema learning for robotic manipulators from visual self-perception,” 2009. [Online]. Available: <https://www.semanticscholar.org/paper/c8982c68d7f7cace3375a875cb895a307d5b89dd>
- [43] S. Fuke, M. Ogino, and M. Asada, “Body image constructed from motor and tactile images with visual information,” *Int. J. Humanoid Robotics*, vol. 4, no. 2, pp. 347–364, 2007.
- [44] K. Malinovska, I. Farkas, J. Harvanova, and M. Hoffmann, “A connectionist model of associating proprioceptive and tactile modalities in a humanoid robot,” 2022.
- [45] P. D. H. Nguyen, M. Hoffmann, U. Pattacini, and G. Metta, “Reaching development through visuo-proprioceptive-tactile integration on a humanoid robot - a deep learning approach,” 2019.

- [46] G. Pugach, A. Pitti, O. Tolochko, and P. Gaussier, "Brain-inspired coding of robot body schema through visuo-motor integration of touched events," *Frontiers Neurorobotics*, vol. 13, p. 5, 2019.
- [47] P. Lanillos, E. Dean-Leon, and G. Cheng, "Yielding self-perception in robots through sensorimotor contingencies," *IEEE Transactions on Cognitive and Developmental Systems*, vol. 9, no. 2, pp. 100–112, 2016.
- [48] J. M. Hollerbach and C. W. Wampler, "The calibration index and taxonomy for robot kinematic calibration methods," *The International Journal of Robotics Research*, vol. 15, no. 6, pp. 573–591, 1996.
- [49] J. Swevers, W. Verdonck, and J. De Schutter, "Dynamic model identification for industrial robots," *IEEE Control Systems*, vol. 27, no. 5, pp. 58–71, 2007.
- [50] Q. Leboutet, J. Roux, A. Janot, J. R. Guadarrama-Olvera, and G. Cheng, "Inertial parameter identification in robotics: A survey," *Applied Sciences*, vol. 11, no. 9, p. 4303.
- [51] K. Ayusawa, G. Venture, and Y. Nakamura, "Identifiability and identification of inertial parameters using the underactuated base-link dynamics for legged multibody systems," *The International Journal of Robotics Research*, vol. 33, no. 3, pp. 446–468, sep 2 2014.
- [52] A. C.-H. Lee, H.-K. Hsu, and H.-P. Huang, "Optimized system identification of humanoid robots with physical consistency constraints and floating-based exciting motions," *International Journal of Humanoid Robotics*, vol. 19, no. 05, p. 2250015, 2022.
- [53] J. Bongard, V. Zykov, and H. Lipson, "Automated synthesis of body schema using multiple sensor modalities," in *Proc. of the Int. Conf. on the Simulation and Synthesis of Living Systems (ALIFEX)*. Citeseer, 2006.
- [54] ——, "Resilient machines through continuous self-modeling," *Science*, vol. 314, no. 5802, pp. 1118–1121, 2006.
- [55] M. Tsakiris, "The multisensory basis of the self: From body to identity to others," *Quarterly Journal of Experimental Psychology* (2006), vol. 70, pp. 597 – 609, 2016. [Online]. Available: <https://api.semanticscholar.org/CorpusID:13628625>
- [56] M. S. Overgaard, C. Preston, and J. E. Aspell, "The self, its body and its brain," *Scientific Reports*, vol. 13, 2023. [Online]. Available: <https://api.semanticscholar.org/CorpusID:260701746>

- [57] J. Wainer, D. Feil-Seifer, D. A. Shell, and M. J. Matarić, “The role of physical embodiment in human-robot interaction,” *ROMAN 2006 - The 15th IEEE International Symposium on Robot and Human Interactive Communication*, pp. 117–122, 2006. [Online]. Available: <https://api.semanticscholar.org/CorpusID:12556718>
- [58] R. Der, *On the Role of Embodiment for Self-Organizing Robots: Behavior As Broken Symmetry*. Berlin, Heidelberg: Springer Berlin Heidelberg, 2014, pp. 193–221. [Online]. Available: [https://doi.org/10.1007/978-3-642-53734-9\\_7](https://doi.org/10.1007/978-3-642-53734-9_7)
- [59] B. R. Duffy and G. Joue, “Intelligent robots: The question of embodiment,” in *Proc. of the Brain-Machine Workshop*. Citeseer, 2000.
- [60] B. Lara, D. Astorga, E. Mendoza-Bock, M. Pardo, E. Escobar, and A. Ciria, “Embodied cognitive robotics and the learning of sensorimotor schemes,” *Adaptive Behavior*, vol. 26, pp. 225 – 238, 2018. [Online]. Available: <https://api.semanticscholar.org/CorpusID:52878823>
- [61] B. Miller and D. Feil-Seifer, “Embodiment, situatedness, and morphology for humanoid robots interacting with people,” *Humanoid Robotics: A Reference*, 2018. [Online]. Available: <https://api.semanticscholar.org/CorpusID:53131244>
- [62] R. Pfeifer, “Morphological computation - connecting brain, body, and environment,” in *Australian Conference on Artificial Intelligence*, 2006. [Online]. Available: <https://api.semanticscholar.org/CorpusID:17211122>
- [63] G. Pezzulo, L. W. Barsalou, A. Cangelosi, M. H. Fischer, K. McRae, and M. J. Spivey, “Computational grounded cognition: a new alliance between grounded cognition and computational modeling,” *Frontiers in Psychology*, vol. 3, 2013. [Online]. Available: <https://api.semanticscholar.org/CorpusID:2597623>
- [64] R. A. Brooks, “New approaches to robotics,” *Science*, vol. 253, pp. 1227 – 1232, 1991. [Online]. Available: <https://api.semanticscholar.org/CorpusID:7385037>
- [65] R. Pfeifer, M. Lungarella, and F. Iida, “Self-organization, embodiment, and biologically inspired robotics,” *Science*, vol. 318, pp. 1088 – 1093, 2007. [Online]. Available: <https://api.semanticscholar.org/CorpusID:13363604>
- [66] A. Maravita, C. Spence, and J. Driver, “Multisensory integration and the body schema: Close to hand and within reach,” *Current Biology*, 2003.
- [67] M. Asada, “Proprioception and body schema,” in *Living machines: A handbook of research in biomimetics and biohybrid systems*. Oxford University Press, 04 2018. [Online]. Available: <https://doi.org/10.1093/oso/9780199674923.003.0018>

- [68] F. de Vignemont, "Body schema and body image—pros and cons," *Neuropsychologia*, vol. 48, pp. 669–680, 2010. [Online]. Available: <https://api.semanticscholar.org/CorpusID:16746475>
- [69] J. Medina and H. B. Coslett, "From maps to form to space: Touch and the body schema," *Neuropsychologia*, vol. 48, pp. 645–654, 2010. [Online]. Available: <https://api.semanticscholar.org/CorpusID:264649687>
- [70] F. d. Vignemont, V. Pitron, and A. J. T. Alsmith, "3C1What is the body schema?" in *Body Schema and Body Image: New Directions*. Oxford University Press, 07 2021. [Online]. Available: <https://doi.org/10.1093/oso/9780198851721.003.0001>
- [71] P. Morasso, M. Casadio, V. Mohan, F. Rea, and J. Zenzeri, "Revisiting the body-schema concept in the context of whole-body postural-focal dynamics," *Frontiers in human neuroscience*, vol. 9, p. 83, 2015.
- [72] R. Grush, "The emulation theory of representation: Motor control, imagery, and perception," *Behavioral and Brain Sciences*, vol. 27, pp. 377 – 396, 2004. [Online]. Available: <https://api.semanticscholar.org/CorpusID:514252>
- [73] J. W. Hart and B. Scassellati, "Robotic self-models inspired by human development," in *Workshops at the Twenty-Fourth AAAI Conference on Artificial Intelligence*, 2010.
- [74] J. Sturm, C. Plagemann, and W. Burgard, "Body schema learning," in *Towards Service Robots for Everyday Environments*. Springer, 2012, pp. 131–161.
- [75] S. Warren, N. F. Capra, and R. Yezierski, "The somatosensory system i: Tactile discrimination and position sense," 2018. [Online]. Available: <https://api.semanticscholar.org/CorpusID:92270180>
- [76] M. Hoffmann, "Body models in humans, animals, and robots: mechanisms and plasticity," *Body Schema and Body Image: New Directions*, pp. 152–180, 2021.
- [77] J. M. Kenzie, J. A. Semrau, M. D. Hill, S. H. Scott, and S. P. Dukelow, "A composite robotic-based measure of upper limb proprioception," *Journal of NeuroEngineering and Rehabilitation*, vol. 14, 2017. [Online]. Available: <https://api.semanticscholar.org/CorpusID:5869217>
- [78] U. Proske and S. C. Gandevia, "The proprioceptive senses: their roles in signaling body shape, body position and movement, and muscle force," *Physiological reviews*, 2012.
- [79] E. D'Antonio, E. Galofaro, J. Zenzeri, F. Patané, J. Konczak, M. Casadio, and L. Masia, "Robotic assessment of wrist proprioception during kinaesthetic perturbations: A

- neuroergonomic approach," *Frontiers in Neurorobotics*, vol. 15, 2021. [Online]. Available: <https://api.semanticscholar.org/CorpusID:232070377>
- [80] S. Hillier, M. Immink, and D. Thewlis, "Assessing proprioception: A systematic review of possibilities," *Neurorehabilitation and Neural Repair*, vol. 29, no. 10, pp. 933–949, 2015, pMID: 25712470. [Online]. Available: <https://doi.org/10.1177/1545968315573055>
- [81] L. Cardinali, C. Brozzoli, J. Luauté, A. C. Roy, and A. Farnè, "Proprioception is necessary for body schema plasticity: evidence from a deafferented patient," *Frontiers in Human Neuroscience*, vol. 10, p. 272, 2016.
- [82] R. Siegwart, I. R. Nourbakhsh, and D. Scaramuzza, *Introduction to autonomous mobile robots*. MIT press, 2011.
- [83] K. M. Lynch and F. C. Park, *Modern robotics*. Cambridge University Press, 2017.
- [84] M. Xie, "Fundamentals of robotics - linking perception to action," in *Series in Machine Perception and Artificial Intelligence*, 2003. [Online]. Available: <https://api.semanticscholar.org/CorpusID:11301738>
- [85] B. Siciliano, L. Sciavicco, L. Villani, and G. Oriolo, "Robotics: Modelling, planning and control," 2008. [Online]. Available: <https://api.semanticscholar.org/CorpusID:109962001>
- [86] J. J. Craig, "Introduction to robotics - mechanics and control (2. ed.)," 1989. [Online]. Available: <https://api.semanticscholar.org/CorpusID:40305864>
- [87] R. Featherstone, "Rigid body dynamics algorithms," 2007. [Online]. Available: <https://api.semanticscholar.org/CorpusID:58437819>
- [88] Chen-Gang, Li-tong, Chu-Ming, J.-Q. Xuan, and S.-H. Xu, "Review on kinematics calibration technology of serial robots," *International Journal of Precision Engineering and Manufacturing*, vol. 15, pp. 1759–1774, 2014. [Online]. Available: <https://api.semanticscholar.org/CorpusID:110728565>
- [89] T. Petrič and L. Žlajpah, "Kinematic model calibration of a collaborative redundant robot using a closed kinematic chain," *Scientific Reports*, vol. 13, 2023. [Online]. Available: <https://api.semanticscholar.org/CorpusID:264304454>
- [90] C. G. Atkeson, C. H. An, and J. M. Hollerbach, "Estimation of inertial parameters of manipulator loads and links," *The International Journal of Robotics Research*, vol. 5, no. 3, pp. 101–119, 1986.

- [91] B. Siciliano and O. Khatib, "Springer handbook of robotics," in *Springer Handbooks*, 2007. [Online]. Available: <https://api.semanticscholar.org/CorpusID:35379589>
- [92] M. Gautier and W. Khalil, "Exciting trajectories for robot inertial parameters identification," *IFAC Proceedings Volumes*, vol. 25, pp. 585–590, 1992. [Online]. Available: <https://api.semanticscholar.org/CorpusID:115399245>
- [93] K.-J. Park, "Fourier-based optimal excitation trajectories for the dynamic identification of robots," *Robotica*, vol. 24, no. 5, pp. 625–633, 2006.
- [94] W. Khalil and E. Dombre, *Modeling, identification and control of robots*. Butterworth-Heinemann, 2004.
- [95] K. Ayusawa, G. Venture, and Y. Nakamura, "Identification of humanoid robots dynamics using floating-base motion dynamics," in *Intelligent Robots and Systems, 2008. IROS 2008. IEEE/RSJ International Conference on*. IEEE, 2008, pp. 2854–2859.
- [96] ——, "Identification of the inertial parameters of a humanoid robot using unactuated dynamics of the base link," in *Humanoid Robots, 2008. Humanoids 2008. 8th IEEE-RAS International Conference on*. IEEE, 2008, pp. 1–7.
- [97] ——, "Minimal-set of Inertial Parameters Identification of Legged Robots Using Base-link Dynamics," *Journal of the Robotics Society of Japan*, vol. 27, no. 9, pp. 1066–1077, 2009.
- [98] T. Iwasaki, G. Venture, and E. Yoshida, "Identification of the inertial parameters of a humanoid robot using grounded sole link," in *2012 12th IEEE-RAS International Conference on Humanoid Robots (Humanoids 2012)*. IEEE, 11 2012.
- [99] J. Jovic, A. Escande, K. Ayusawa, E. Yoshida, A. Kheddar, and G. Venture, "Humanoid and Human Inertia Parameter Identification Using Hierarchical Optimization," *IEEE Transactions on Robotics*, vol. 32, no. 3, pp. 726–735, 6 2016.
- [100] M. Mistry, S. Schaal, and K. Yamane, "Inertial parameter estimation of floating base humanoid systems using partial force sensing," in *Humanoid Robots, 2009. Humanoids 2009. 9th IEEE-RAS International Conference on*. IEEE, 12 2009, pp. 492–497.
- [101] R. Hartley, J. Mangelson, L. Gan, M. Ghaffari Jadidi, J. M. Walls, R. M. Eustice, and J. W. Grizzle, "Legged Robot State-Estimation Through Combined Forward Kinematic and Preintegrated Contact Factors," in *2018 IEEE International Conference on Robotics and Automation (ICRA)*. IEEE, 5 2018.

- [102] Russell Buchanan, Marco Camurri, F. Dellaert, and M. Fallon, “Learning Inertial Odometry for Dynamic Legged Robot State Estimation,” *Conference on Robot Learning*, 2021.
- [103] W. Khalil, F. Boyer, and F. Morsli, “General Dynamic Algorithm for Floating Base Tree Structure Robots With Flexible Joints and Links,” *Journal of Mechanisms and Robotics*, vol. 9, no. 3, p. 031003, 03 2017. [Online]. Available: <https://doi.org/10.1115/1.4035798>
- [104] P. M. Wensing, S. Kim, and J.-J. E. Slotine, “Linear matrix inequalities for physically consistent inertial parameter identification: A statistical perspective on the mass distribution,” *IEEE Robotics and Automation Letters*, vol. 3, no. 1, pp. 60–67, 2017.
- [105] K. Ayusawa and Y. Nakamura, “Identification of standard inertial parameters for large-dof robots considering physical consistency,” in *2010 IEEE/RSJ International Conference on Intelligent Robots and Systems*. IEEE, 2010, pp. 6194–6201.
- [106] S. Traversaro, S. Brossette, A. Escande, and F. Nori, “Identification of fully physical consistent inertial parameters using optimization on manifolds,” in *2016 IEEE/RSJ International Conference on Intelligent Robots and Systems (IROS)*. IEEE, 2016, pp. 5446–5451.
- [107] C. D. Sousa and R. Cortesão, “Physical feasibility of robot base inertial parameter identification: A linear matrix inequality approach,” *The International Journal of Robotics Research*, vol. 33, no. 6, pp. 931–944, 2014.
- [108] S. Jayasumana, R. Hartley, M. Salzmann, H. Li, and M. Harandi, “Kernel methods on the riemannian manifold of symmetric positive definite matrices,” in *Proceedings of the IEEE Conference on Computer Vision and Pattern Recognition*, 2013, pp. 73–80.
- [109] X. Pennec, P. Fillard, and N. Ayache, “A riemannian framework for tensor computing,” *International Journal of computer vision*, vol. 66, no. 1, pp. 41–66, 2006.
- [110] T. Lee and F. C. Park, “A geometric algorithm for robust multibody inertial parameter identification,” *IEEE Robotics and Automation Letters*, vol. 3, no. 3, pp. 2455–2462, 2018.
- [111] R. Pfeifer, M. Lungarella, O. Sporns, and Y. Kuniyoshi, “On the information theoretic implications of embodiment - principles and methods,” in *50 Years of Artificial Intelligence*, 2006. [Online]. Available: <https://api.semanticscholar.org/CorpusID:735241>
- [112] M. Lungarella and O. Sporns, “Embodiment, information, and causal structure.”

- [113] N. M. Schmidt, M. Hoffmann, K. Nakajima, and R. Pfeifer, “Bootstrapping perception using information theory: Case studies in a quadruped robot running on different grounds,” *Advances in Complex Systems*, vol. 16, no. 02n03, p. 1250078, 2013.
- [114] M. Lungarella and O. Sporns, “Mapping information flow in sensorimotor networks,” *PLoS Comput Biol*, vol. 2, no. 10, p. e144, 2006.
- [115] D. Polani and M. Möller, “Models of information processing in the sensorimotor loop,” in *Information Theory and Statistical Learning*. Springer, 2009, pp. 289–308.
- [116] T. Bossomaier, L. Barnett, M. Harré, and J. T. Lizier, “An introduction to transfer entropy,” *Cham: Springer International Publishing*, vol. 65, 2016.
- [117] L. A. Olsson, C. L. Nehaniv, and D. Polani, “From unknown sensors and actuators to actions grounded in sensorimotor perceptions,” *Connection Science*, vol. 18, no. 2, pp. 121–144, 2006.
- [118] D. B. West *et al.*, *Introduction to graph theory*. Prentice hall Upper Saddle River, 2001, vol. 2.
- [119] G. Mateos, S. Segarra, A. G. Marques, and A. Ribeiro, “Connecting the dots: Identifying network structure via graph signal processing,” *IEEE Signal Processing Magazine*, vol. 36, no. 3, pp. 16–43, 2019.
- [120] D. Spielman, “Spectral graph theory,” *Combinatorial scientific computing*, vol. 18, p. 18, 2012.
- [121] R. Sefidgar, “The minimum spanning tree algorithm.” [Online]. Available: [https://algorithms.discrete.ma.tum.de/graph-algorithms/mst-kruskal/index\\_en.html](https://algorithms.discrete.ma.tum.de/graph-algorithms/mst-kruskal/index_en.html)
- [122] A. Kershenbaum and R. Van Slyke, “Computing minimum spanning trees efficiently,” in *Proceedings of the ACM annual conference-Volume 1*, 1972, pp. 518–527.
- [123] B. Crawford, R. Gera, J. House, T. Knuth, and R. Miller, “Graph structure similarity using spectral graph theory,” in *Complex Networks & Their Applications V*, H. Cherifi, S. Gaito, W. Quattrociocchi, and A. Sala, Eds. Cham: Springer International Publishing, 2017, pp. 209–221.
- [124] R. Gera, L. Alonso, B. Crawford, J. House, J. A. Mendez-Bermudez, T. Knuth, and R. Miller, “Identifying network structure similarity using spectral graph theory,” *Applied Network Science*, vol. 3, no. 1, pp. 1–15, 1 2018. [Online]. Available: <http://link.springer.com/article/10.1007/s41109-017-0042-3>

- [125] P. Wills and F. G. Meyer, "Metrics for graph comparison: a practitionerâ€™s guide," *PloS one*, vol. 15, no. 2, p. e0228728, 2020.
- [126] X. Dong, D. Thanou, M. Rabbat, and P. Frossard, "Learning graphs from data: A signal representation perspective," *IEEE Signal Processing Magazine*, vol. 36, no. 3, pp. 44–63, 2019.
- [127] W. Karwowski, F. Vasheghani Farahani, and N. Lighthall, "Application of graph theory for identifying connectivity patterns in human brain networks: a systematic review," *frontiers in Neuroscience*, vol. 13, p. 585, 2019.
- [128] H.-J. Park and K. Friston, "Structural and functional brain networks: from connections to cognition," *Science*, vol. 342, no. 6158, 2013.
- [129] J. Faskowitz, R. F. Betzel, and O. Sporns, "Edges in brain networks: Contributions to models of structure and function," *Network Neuroscience*, pp. 1–28.
- [130] K. J. Friston, "Functional and effective connectivity: a review," *Brain connectivity*, vol. 1, no. 1, pp. 13–36, 2011.
- [131] A. M. Bastos and J.-M. Schoffelen, "A tutorial review of functional connectivity analysis methods and their interpretational pitfalls," *Frontiers in systems neuroscience*, vol. 9, p. 175, 2016.
- [132] W. Zhang, J. Chien, J. Yong, and R. Kuang, "Network-based machine learning and graph theory algorithms for precision oncology," *NPJ precision oncology*, vol. 1, no. 1, pp. 1–15, 2017.
- [133] O. Sporns, "Graph theory methods: applications in brain networks," *Dialogues in clinical neuroscience*, vol. 20, no. 2, p. 111, 2018.
- [134] L. Stanković, M. Daković, and E. Sejdić, "Introduction to graph signal processing," in *Vertex-Frequency Analysis of Graph Signals*. Springer, 2019, pp. 3–108.
- [135] R. Mazumder and T. J. Hastie, "The graphical lasso: New insights and alternatives," *Electronic journal of statistics*, vol. 6, pp. 2125–2149, 2011. [Online]. Available: <https://api.semanticscholar.org/CorpusID:6795998>
- [136] H. E. Egilmez. (2021) Graph laplacian learning (GLL) package v2.1. [Online]. Available: [https://github.com/STAC-USC/Graph\\_Learning](https://github.com/STAC-USC/Graph_Learning)
- [137] A. F. Villaverde, J. Ross, F. Morán, and J. R. Banga, "Mider: network inference with mutual information distance and entropy reduction," *Plos one*, vol. 9, no. 5, p. e96732, 2014.

- [138] M. Ursino, G. Ricci, and E. Magosso, “Transfer entropy as a measure of brain connectivity: A critical analysis with the help of neural mass models,” *Frontiers in Computational Neuroscience*, vol. 14, p. 45, 2020.
- [139] L. Novelli and J. T. Lizier, “Inferring network properties from time series via transfer entropy and mutual information: validation of bivariate versus multivariate approaches,” *CoRR*, vol. abs/2007.07500, 2020. [Online]. Available: <https://arxiv.org/abs/2007.07500>
- [140] T. M. Cover, *Elements of information theory*. John Wiley & Sons, 1999.
- [141] N. M. Timme and C. Lapish, “A tutorial for information theory in neuroscience,” *eneuro*, vol. 5, no. 3, 2018.
- [142] L. Bottou, “Stochastic gradient descent tricks,” in *Neural Networks: Tricks of the Trade: Second Edition*. Springer, 2012, pp. 421–436.
- [143] Y. Tian, Y. Zhang, and H. Zhang, “Recent advances in stochastic gradient descent in deep learning,” *Mathematics*, vol. 11, no. 3, p. 682, 2023.
- [144] S. Ruder, “An overview of gradient descent optimization algorithms,” *ArXiv*, vol. abs/1609.04747, 2016. [Online]. Available: <https://api.semanticscholar.org/CorpusID:17485266>
- [145] D. P. Kingma and J. Ba, “Adam: A method for stochastic optimization,” *arXiv preprint arXiv:1412.6980*, 2014.
- [146] S. J. Reddi, S. Kale, and S. Kumar, “On the convergence of ADAM and beyond,” *arXiv preprint arXiv:1904.09237*, 2019.
- [147] N. Boumal, “Optimization and estimation on manifolds.” Ph.D. dissertation, Catholic University of Louvain, Louvain-la-Neuve, Belgium, 2014.
- [148] D. Brooks, O. Schwander, F. Barbaresco, J.-Y. Schneider, and M. Cord, “Riemannian batch normalization for spd neural networks,” in *Advances in Neural Information Processing Systems*, 2019, pp. 15 463–15 474.
- [149] S. Bonnabel, “Stochastic gradient descent on riemannian manifolds,” *IEEE Transactions on Automatic Control*, vol. 58, no. 9, pp. 2217–2229, 2013.
- [150] G. Bécigneul and O.-E. Ganea, “Riemannian adaptive optimization methods,” *arXiv preprint arXiv:1810.00760*, 2018.